

# Heterodimetallic Chalcogen-Bridged Cubane-Type Clusters of Molybdenum and Tungsten Containing First-Row Transition Metals

Rosa Llusar<sup>\*[a]</sup> and Santiago Uriel<sup>[b]</sup>

**Keywords:** Molybdenum / Tungsten / Cluster compounds / Sulfur / Selenium / Heterometallic complexes

Transition metal cluster chalcogenides with cubane-type structures are relevant to our understanding of several industrial and biological catalytic processes. Recent advances in cluster chemistry owe much to the development of rational synthetic approaches, an aspect that is emphasised in this review which focuses on cuboidal clusters of molybdenum and tungsten (M) with  $M_2M'_2S_4$  and  $M_3M'_3Q_4$  (Q = S, Se) central units that incorporate a first-row transition metal atom (M'). Special attention has been paid to the non-aque-

ous chemistry of these compounds. The structural features of these complexes are discussed in relation to their electronic structures within the framework of molecular orbital theory, spectroscopic, magnetic and electrochemical experimental data. Finally, the importance of these clusters in catalysis, nonlinear optics and in the formation of supramolecular adducts is discussed.

(© Wiley-VCH Verlag GmbH & Co. KGaA, 69451 Weinheim, Germany, 2003)

## Introduction

Transition metal chalcogenide clusters with a cubane-type structure, where the metal and chalcogen atoms occupy adjacent vertices in a cube, are a unique area within cluster chemistry. These compounds are of interest not only

because of their contribution to the development of modern chemistry, but also for their potential use as models for various industrial and biological catalytic processes.<sup>[1–3]</sup> In addition, these complexes have recently been utilised as optical limiters and contrast agents.<sup>[4–7]</sup>

The first cuboidal cluster to be identified contained the  $Fe_4S_4$  core, a redox-active unit present in the electron-transfer protein ferredoxin. In addition to this homonuclear system, several important metalloenzymes contain heteronuclear transition metal sites. For example, nitrogenase contains the unique Fe-Mo cofactor, which is a major part of the dinitrogen activation system. The characterisation of the Fe-Mo cofactor by X-ray diffraction techniques has

<sup>[a]</sup> Departament de Ciències Experimentals, Universitat Jaume I, Campus de Riu Sec, P. O. Box 224, 12080 Castelló, Spain  
Fax: (internat.) + 34-964/728066  
E-mail: llusar@exp.uji.es

<sup>[b]</sup> Departamento de Química Orgánica – Química Física, Centro Politécnico Superior, Universidad de Zaragoza, María de Luna 3, 50015 Zaragoza, Spain  
Fax: (internat.) + 34-976/761879  
E-mail: suriel@posta.unizar.es



Rosa Llusar was born in Almenara (Spain). She studied chemistry at the University of Valencia (Spain) and received Ph.D. degrees from Valencia University in 1987 and from Texas A&M University (USA) in 1988 under the guidance of Prof. F. Albert Cotton. After working for industry for three years, she spent one year (1992) with Prof. John D. Corbett at the Ames Laboratory (Iowa State University, USA). Since 1993, she has held a position at the University Jaume I of Castelló (Spain) and became Associate Professor of Physical Chemistry in 1995. Her research has focussed on the chemistry of transition metal clusters, especially the relationship between their molecular and electronic structures and their properties.



Santiago Uriel was born in Madrid (Spain). He received his PhD degree in 1992 from Zaragoza University. His doctoral work, under the supervision of Dr. J. Garín, dealt with the synthesis of new (aminomethyl)tetrathiafulvalene derivatives. He then spent three years with Dr. Patrick Batail, first at Laboratoire de Physique des Solides of the University of Paris XI (Orsay) supported by an E. U. Human Capital and Mobility fellowship, and subsequently at the Institut de Matériaux de Nantes as Research Associate at the Centre National de la Recherche Scientifique. He worked on the molecular chemistry of octahedral rhenium clusters and their association within organic-inorganic materials. He joined the research group of Dr. R. Llusar in 1997 at the Jaume I University of Castellón (Spain) supported by Ministerio de Educación y Ciencia and he is currently Profesor Asociado at the Organic Chemistry Department of the University of Zaragoza. His research interests include synthesis, structural chemistry and physical properties of transition metal molecular ions.

**MICROREVIEWS:** This feature introduces the readers to the authors' research through a concise overview of the selected topic. Reference to important work from others in the field is included.

shown the presence of a  $\text{MoFe}_7\text{S}_8$  core structure with two partial thiocubane substructures, each of which contains an open  $\text{Fe}_3$  face.<sup>[8,9]</sup> Synthetic efforts to prepare chemical analogues of the cofactor have been extensively reviewed and will not be covered here.<sup>[10,11]</sup>

This review is limited to heterodimetallic cuboidal  $\text{M}_2\text{M}'_2$  and  $\text{M}_3\text{M}'$  cluster chalcogenides of molybdenum and tungsten (M) that incorporate a first-row transition metal ( $\text{M}'$ ). Heterodimetallic clusters with  $\text{M}_2\text{M}'_2\text{S}_4$  and  $\text{M}_3\text{M}'\text{S}_4$  cores ( $\text{M}' = \text{Ni}, \text{Co}$ ) are considered as discrete molecular models for substrate binding in the hydrodesulfurisation process (HDS), due to the fact that cobalt and nickel are known to act as promoters of the catalytic activity of the molybdenum sulfide industrial heterogeneous catalysts.<sup>[12]</sup> Sulfur- or selenium-containing transition metal clusters with  $\text{MM}'_3\text{S}_3\text{Br}$  or  $\text{M}_3\text{M}'\text{Se}_4$  ( $\text{M} = \text{Mo}$  and  $\text{W}$ ;  $\text{M}' = \text{Cu}$  and  $\text{Ag}$ ) cubane-like structures are also known to possess strong optical limiting effects.<sup>[4,5,13,14]</sup> In the past ten years, several review articles have appeared covering the most important aspects of the chemistry of molybdenum and tungsten transition metal chalcogenides.<sup>[1,15–19]</sup> Special attention has been given to the aqueous chemistry of heterodimetallic molybdenum and tungsten  $\text{M}_3\text{M}'\text{Q}_4$  clusters that incorporate a second transition metal atom.<sup>[1,15,17,18]</sup>

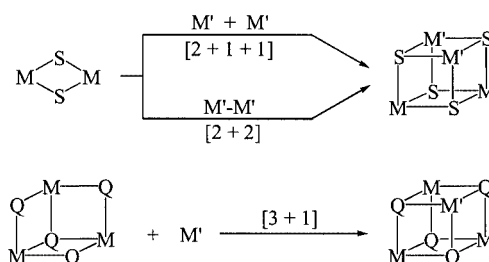
In this work we place our emphasis on the non-aqueous chemistry of these complexes, a field of particular interest to us. In addition, we have included results reported on the  $\text{M}_2\text{M}'_2\text{S}_4$  systems for comparative purposes. We have restricted  $\text{M}'$  to the first-row transition elements, again motivated by our own research interests. The review is organised as follows. The first section provides a general overview of the synthesis, structure and electron counts of clusters with  $\text{M}_2\text{M}'_2\text{S}_4$  and  $\text{M}_3\text{M}'\text{Q}_4$  central units. Each subsection is defined based on the nature of the surrounding ligands around the group-6 metal atom. The next section discusses the electronic structure, electrochemistry and magnetism of these  $\text{M}_2\text{M}'_2\text{S}_4$  and  $\text{M}_3\text{M}'\text{Q}_4$  clusters. The final section deals with some selected properties that we have decided to emphasise, based on their potential applications such as catalysis, nonlinear optics and the capability of these cluster compounds to form supramolecular adducts.

## Synthesis, Structure and Electron Counts

The development of the chemistry of transition metal clusters is closely related to the discovery of rational synthetic routes for the preparation of these compounds. In recent years, different strategies have evolved for the synthesis of molecular transition metal sulfide systems. These strategies can be roughly classified into six different categories: (i) spontaneous self-assembly where the structure of the reactant is not preserved in the final product; (ii) fragmentation of clusters of higher nuclearity; (iii) cluster excision from solid-state polymers; (iv) building-block synthesis from lower nuclearity species; (v) transmetallation or replacement of one metal atom by another, and (vi) substi-

tution of peripheral ligands. The first two procedures suffer from the disadvantage that the structures of the products cannot be easily predicted.

The building-block approach has been the most widely used method for the construction of cuboidal heterodimetallic  $\text{M}_2\text{M}'_2\text{S}_4$  and  $\text{M}_3\text{M}'\text{Q}_4$  ( $\text{Q} = \text{S}, \text{Se}$ ) cluster complexes. Using this approach,  $\text{M}_2\text{M}'_2\text{S}_4$  complexes can be prepared from a dinuclear precursor and two mononuclear complexes according to the so-called  $[2 + 1 + 1]$  route, or from two dinuclear compounds according to a strategy designated as  $[2 + 2]$ .  $\text{M}_3\text{M}'\text{Q}_4$  clusters can be prepared in an analogous fashion by adding a monomeric compound to a triangular metal complex, this method being termed a  $[3 + 1]$  synthesis. Scheme 1 gives a graphical representation of these three methods.



Scheme 1. Building-block synthetic methods for heterometallic cubane clusters

Once the heterodimetallic tetrameric unit has been formed, it can undergo different chemical transformations without changing its nuclearity. For example, one of the metal atoms can be substituted for a different metal atom (transmetallation) or the outer ligands can be replaced by other ligands (ligand substitution). In addition, the structure of the cluster core can rearrange in the presence of certain reagents.

The trinuclear and dinuclear precursors have been prepared by a variety of methods such as self-assembly, cluster fragmentation and cluster excision. This last method has represented a major advance in the field because it both allows the synthesis of previously inaccessible compounds and gives significant improvements in the yields of the cluster formation reactions. In this section we will first present details of the synthesis of the dinuclear or trinuclear precursors for each particular group of compounds, and then continue with a general description of the synthesis employed to obtain  $\text{M}_2\text{M}'_2\text{S}_4$  and  $\text{M}_3\text{M}'\text{Q}_4$  cluster complexes.

### Clusters with $\text{M}_2\text{M}'_2\text{S}_4$ Central Units

A simplified representation of the structures of representative compounds with  $\text{Mo}_2\text{M}'_2\text{S}_4$  and  $\text{W}_2\text{M}'_2\text{S}_4$  cluster units is given in Figure 1. All structures have been drawn to emphasise the familiar thiocubane core and the coordination environments of the metal atoms. No analogous compounds of selenium have yet been reported to our knowledge. A summary of intermetallic distances for some representative cluster compounds within this series is given in Table 1.

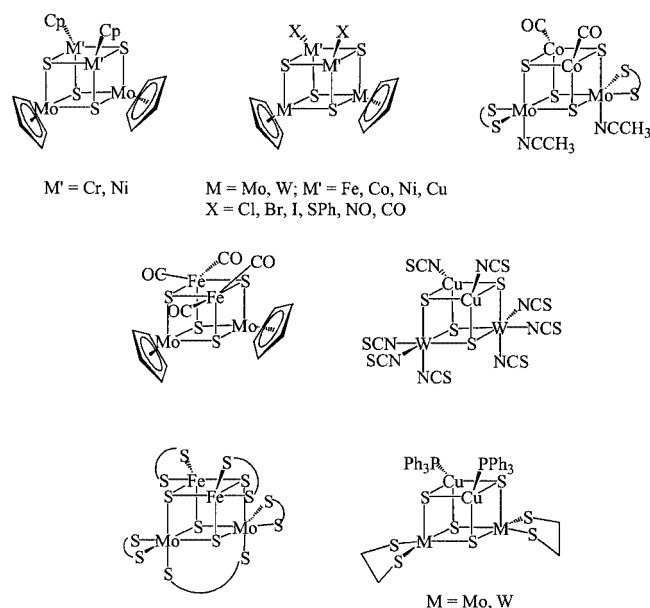


Figure 1. Schematic representations of the different coordination environments in  $M_2M'_2S_4$  cubane-type clusters

Dimeric molybdenum and tungsten sulfur-rich complexes with cyclopentadienyl (Cp) and sulfur-containing ligands (dithiocarbamates, 1,2-dimercaptoethane or polysulfides) have been used as precursors for the synthesis of heterometallic  $M_2M'_2S_4$  clusters through [2 + 1 + 1] or [2 + 2] building block strategies. These complexes behave as metalloli-

gands towards heterometal atoms by using the lone-pair electrons of the sulfur atoms. The most widely used building block is the  $M_2S_4$  unit, particularly the molybdenum- and tungsten(v)  $[M_2S_2(\mu_2-S)_2]$  isomeric forms. Note however, that the tetrabridged molybdenum(IV) complex  $[Mo_2(\mu_2-S)_2(\mu_2-SH)_2Cp_2]$  is often used for the synthesis of (cyclopentadienyl)molybdenum derivatives. The heterometal  $M'$  is usually incorporated as a mononuclear or a dinuclear carbonyl complex except in the case of copper, where incorporation has always been accomplished by reaction with copper halides. The coordination environment of the heteroatom depends on the composition of the carbonylmetal compound.

### $M_2M'_2S_4$ Clusters with Cyclopentadienyl Ligands

The dinuclear cyclopentadienyl building blocks  $[M_2S_4Cp_2]$  are prepared by reaction of the molybdenum(I) or the tungsten(I) dinuclear complex  $[MCp^*(CO)_2]_2$  with elemental sulfur in refluxing toluene to produce a mixture of isomers with metal atoms in oxidation states ranging from III to V.<sup>[34]</sup> The product distribution depends on the reaction conditions. Typical reaction yields for the  $[M_2S_4Cp_2]$  dimer are 40% for Mo and 60% for W. In the case of tungsten, the *syn*- $[W_2S_2(\mu_2-S)_2]$  isomer is obtained in 54% yield, while the molybdenum analogue is produced in only 10% yield. Alternatively, the *trans*- $[Mo_2S_2(\mu_2-S)_2Cp^*_2]$  isomer can be prepared in 65% yield by treating the hydridomolybdenum complex  $[MoCp^*H(CO)_3]$  with elemental sulfur in refluxing THF.<sup>[35]</sup> The preparation of the widely used  $[Mo_2(\mu_2-S)_2(\mu_2-SH)_2Cp^*_2]$  precursor is car-

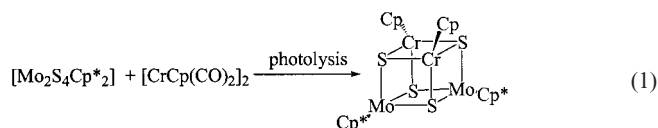
Table 1. Selected bond lengths [Å] and infrared CO or NO stretching frequencies [ $cm^{-1}$ ] for some representative  $Mo_2M'_2S_4$  and  $W_2M'_2S_4$  cubane-type clusters (standard deviations for averaged values are given in brackets)

Cluster	No. of metal electrons	M–M	M–M'	M'–M'	$\nu(CO)$ or $\nu(NO)$ <sup>[a]</sup> <sup>[b]</sup>	Ref.
Mo octahedral and M' tetrahedral coordination:						
$[Mo_2Fe_2S_4Cp^*_2Cl_2]$	16	2.8219(7)	2.757[4]	2.791(1)	—	[20]
$[Mo_2Co_2S_4Cp^*_2Cl_2]$	18	2.804(1)	2.756[5]	2.955(2)	—	[21]
$[Mo_2Co_2S_4Cp^*_2I_2]$	18	2.803(1)	2.738[4]	2.936(1)	—	[21]
$[Mo_2Co_2S_4Cp^*_2(PhS)_2]$	18	2.8156(3)	2.733[1]	2.7414(6)	—	[21]
$[Mo_2Fe_2S_4Cp^*_2(NO)_2]$	20	2.8419(7)	2.7654[7]	2.704(1)	1736/1715	[22]
$[Mo_2Co_2S_4(S_2CNET_2)_2(CH_3CN)_2(CO)_2]$	20	2.788(1)	2.676[6]	2.533(1)	1983/1960	[23]
$[Mo_2Co_2S_4Cp^*_2(CO)_2]$	20	2.8313(5)	2.701[5]	2.5816(9)	1984/1965	[24]
$[Mo_2Co_2S_4Cp^*_2(CO)_2]^-$	21	2.838(1)	2.739[9]	2.746(1)	1898/1865 <sup>[b]</sup>	[25]
$[Mo_2Co_2S_4Cp^*_2(CO)_2]^-$	21	2.846(1)	2.731[6]	2.735(1)	1902/1873 <sup>[b]</sup>	[26]
$[Mo_2Co_2S_4Cp^*_2(NO)_2]$	22	2.8135(6)	2.766[4]	3.116(1)	1747/1717	[22]
$[Mo_2Ni_2S_4Cp^*_2(CO)_2]$	22	2.829(1)	2.722[2]	2.960(1)	1990/1970	[27]
$[Mo_2Cu_2S_4Cp^*_2Cl_2]$	22	2.865(1)	2.788[9]	3.058(3)	—	[28]
Mo octahedral coordination and M' pentacoordinate:						
$[Mo_2Fe_2S_4(\mu-dtc)(dtc)_4]$	15	2.734(2)	2.75[2]	2.784(3)	—	[29]
$[Mo_2Fe_2S_4Cp^*_2(CO)_4]$	18	2.761(1)	2.81[2]	3.334	1995/1962/1934	[30]
Mo pentacoordinate and M' tetrahedral coordination:						
$[Mo_2Cu_2S_4(edt)_2(PPh_3)_2]$	22	2.8576(7)	2.81[2]	3.095(2)	—	[31]
W octahedral and M' tetrahedral coordination:						
$[W_2Fe_2S_4Cp^*_2(NO)_2]$	20	2.8198(9)	2.766[4]	2.735(3)	1736/1715	[22]
$[W_2Co_2S_4Cp^*_2(NO)_2]$	22	2.7984(5)	2.780[4]	3.131(1)	1732/1709	[22]
$[W_2Cu_2S_4(SCN)_8]^{4-}$	22	2.845(2)	2.76[3]	2.999	—	[32]
W pentacoordinate and M' tetrahedral coordination:						
$[W_2Cu_2S_4(edt)_2(PPh_3)_2]$	22	2.851(1)	2.82[2]	3.090	—	[33]

<sup>[a]</sup> All IR data are referred to the CO or NO stretching frequency in KBr unless otherwise indicated. <sup>[b]</sup> IR data in  $CH_3CN$  solutions.

ried out through reduction of the polymeric phase  $\{\text{Mo}_2\text{S}_x\text{Cp}^\#\}_n$  ( $\text{Cp}^\# = \text{Cp}, \text{Cp}', \text{Cp}^*$ ; with  $\text{Cp}' = \text{methylcyclopentadienyl}$  and  $\text{Cp}^* = \text{pentamethylcyclopentadienyl}$ ) with an excess of lithium ethylborohydride.<sup>[36]</sup> This phase is obtained by treating  $[\text{MoCp}^\#(\text{CO})_3]_2$  with elemental sulfur.<sup>[35,37]</sup> The intermetallic distance in  $[\text{Mo}_2(\mu_2\text{-S})_2(\mu_2\text{-SH})_2\text{Cp}_2^\#]$  as well as in  $[\text{M}_2\text{S}_2(\mu_2\text{-S}_2)\text{Cp}_2^\#]$  is consistent with the presence of a metal–metal single bond.

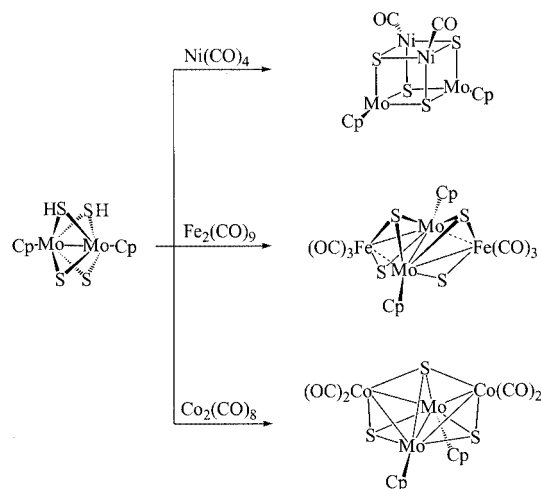
The  $\text{Mo}_2\text{Cr}_2$  core is formed by photolysis of the carbonylchromium(I) complex  $[\text{CrCp}(\text{CO})_2]_2$  in the presence of  $[\text{Mo}_2\text{S}_4\text{Cp}^*_2]$ , which affords the cubane-like diamagnetic cluster  $[\text{Mo}_2\text{Cr}_2\text{S}_4\text{Cp}^*_2\text{Cp}_2]$  in 41% yield according to Equation (1).<sup>[38]</sup>



The equivalent  $[\text{Mo}_2\text{Cr}_2\text{S}_4\text{Cp}_2\text{Cp}^*_2]$  complex has also been prepared by treating a chromium sulfide dimer  $[\text{Cr}_2(\mu_2, \eta^2\text{-S}_2)(\mu_2, \eta^1\text{-S}_2)(\mu_2\text{-S})\text{Cp}^*_2]$  with the corresponding carbonylmolybdenum compound  $[\text{MoCp}(\text{CO})_2]_2$ . The final oxidation state of both Mo and Cr in the cluster is III and consequently there are 12 metal cluster electrons available for metal–metal bonding. The analogous nickel cluster  $[\text{Mo}_2\text{Ni}_2\text{S}_4\text{Cp}'_2\text{Cp}_2]$  has been synthesised in 15% yield from  $[\text{Mo}_2(\mu_2\text{-S})_2(\mu_2\text{-SH})_2\text{Cp}'_2]$  and  $[\text{NiCp}(\text{CO})]_2$  in refluxing THF to produce a 22 metal electron cluster, for which the oxidation state assignment  $\text{Mo}_2^{\text{III}}\text{Ni}_2^{\text{II}}$  has been proposed.<sup>[27]</sup> Consequently, the reaction implies reduction of the dimolybdenum sulfide ( $\text{Mo}^{\text{IV}}$  to  $\text{Mo}^{\text{III}}$ ), with concomitant oxidation of the carbonylnickel compound from  $\text{Ni}^{\text{I}}$  to  $\text{Ni}^{\text{II}}$ . Although these tetrametallic  $\text{Mo}_2\text{Cr}_2\text{S}_4$  and  $\text{Mo}_2\text{Ni}_2\text{S}_4$  clusters have not been characterised by X-ray structural analysis, a cubane-type structure has been proposed based on spectroscopic evidence. The complex  $[\text{Mo}_2(\mu_2\text{-S})_2(\mu_2\text{-SH})_2\text{Cp}'_2]$  does not react with  $[\text{Fe}_2\text{Cp}_2(\text{CO})_4]$  or  $[\text{CoCp}(\text{CO})_2]$  under the conditions used for the synthesis of the  $\text{Mo}_2\text{Ni}_2$  complex.<sup>[27]</sup>

The hydrosulfides  $[\text{Mo}_2(\mu_2\text{-S})_2(\mu_2\text{-SH})_2\text{Cp}^\#_2]$  ( $\text{Cp}^\# = \text{Cp}, \text{Cp}'$ ) react rapidly ( $< 2$  h) with  $[\text{Ni}(\text{CO})_4]$ ,  $[\text{Fe}_2(\text{CO})_9]$  and  $[\text{Co}_2(\text{CO})_8]$  in organic solvents, but only in the case of nickel can  $\text{M}_2\text{M}'_2\text{S}_4$  thiocubane clusters be isolated. These have the formula  $[\text{Mo}_2\text{Ni}_2\text{S}_4\text{Cp}^\#_2(\text{CO})_2]$  and are obtained in 25 and 50% yields for Cp and  $\text{Cp}'$ , respectively, as represented in Scheme 2.<sup>[27,36]</sup>

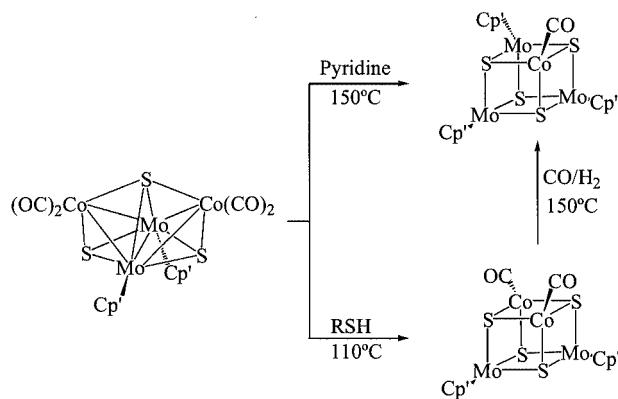
These nickel compounds, also with 22 metal cluster electrons, adopt a cubane-butterfly structure with the Ni atoms placed at the wing tips ( $\text{Ni}\cdots\text{Ni} = 2.962 \text{ \AA}$ ). In the case of iron, the complexes  $[\text{Mo}_2\text{Fe}_2(\mu_3\text{-S})_2(\mu_2\text{-S})_2\text{Cp}^\#_2(\text{CO})_6]$  ( $\text{Cp}^\# = \text{Cp}, \text{Cp}'$ ) are obtained. These contain a planar  $\text{Mo}_2\text{Fe}_2$  core and have the  $\mu_3\text{-S}$  ligands lying on opposite sites of the  $\text{Mo}_2\text{Fe}_2$  plane. Reaction with the carbonylcobalt compound affords the tetranuclear clusters  $[\text{Mo}_2\text{Co}_2(\mu_3\text{-S})_2(\mu_4\text{-S})\text{Cp}^\#_2(\text{CO})_4]$  in 50% yield. These have an  $\text{Mo}_2\text{Co}_2\text{S}_3$  core containing a  $\mu_4\text{-S}$  sulfido ligand. The  $\text{Cp}'$  derivative



Scheme 2. Reactions of  $[\text{Mo}_2(\mu_2\text{-S})_2(\mu_2\text{-SH})_2\text{Cp}_2]$  with carbonylmetal compounds

undergoes thermal decomposition by heating with pyridine at  $150^\circ\text{C}$  to give a trimolybdenum cuboidal cluster  $[\text{Mo}_3\text{CoS}_4\text{Cp}'_3(\text{CO})]$  in 15% yield.<sup>[24]</sup>

The  $[\text{Mo}_2\text{Co}_2(\mu_3\text{-S})_2(\mu_4\text{-S})\text{Cp}'_2(\text{CO})_4]$  complex deserves special attention due to its relevance as a molecular model for hydrodesulfurisation catalysis.<sup>[25,39]</sup> This  $\text{Mo}_2\text{Co}_2\text{S}_3$  cluster compound reacts with a variety of organic thiols  $\text{RSH}$  ( $\text{R} = \text{tert-butyl}, \text{isopentyl}, \text{phenyl}$ ) in near quantitative yield to give the corresponding hydrocarbon and the  $[\text{Mo}_2\text{Co}_2(\mu_3\text{-S})_4\text{Cp}'_2(\text{CO})_2]$  cubane having 20 metal electrons. Treatment of the  $\text{Mo}_2\text{Co}_2\text{S}_4$  cluster with a  $\text{CO}/\text{H}_2$  mixture (1:4) at  $150^\circ\text{C}$  and  $13.4 \times 10^5 \text{ Pa}$  affords the  $[\text{Mo}_3\text{CoS}_4\text{Cp}'_3(\text{CO})]$  complex in 15–30% yield, according to Scheme 3.<sup>[24]</sup>



Scheme 3. Rearrangement reactions of the  $\text{Mo}_2\text{Co}_2\text{S}_3$  core

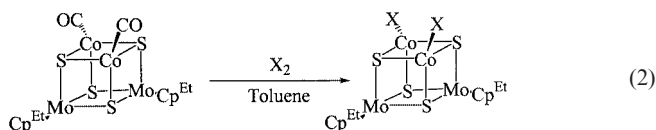
An analogue of  $[\text{Mo}_2\text{Co}_2(\mu_3\text{-S})_4\text{Cp}'_2(\text{CO})_2]$  can be obtained in better yields (72%) from the sulfur-rich dinuclear complex  $[\text{Mo}_2\text{S}_4\text{Cp}^*_2]$  and  $[\text{Co}_2(\text{CO})_8]$  in toluene.<sup>[40]</sup> This procedure can be extended to tungsten to afford the  $[\text{W}_2\text{Co}_2\text{S}_4\text{Cp}^*_2(\text{CO})_2]$  cubane compound in 51% yield.<sup>[22]</sup> The  $\text{M}_2\text{Co}_2\text{S}_4$  cluster unit in these compounds having 20 metal electrons shows a complete metal tetrahedron with six intermetallic bonds (see Table 1), in contrast to the Ni



complex analogue where only five metal–metal bonds are present. If one neglects the intermetallic bonds, the coordination environment around the heterometal in both the Ni and the Co clusters is nearly tetrahedral.

Reduction of the carbonylcobalt cubane  $[\text{Mo}_2\text{Co}_2\text{S}_4\text{Cp}^{\text{Et}}_2(\text{CO})_2]$  ( $\text{Cp}^{\text{Et}}$  = ethyltetramethylcyclopentadienyl) with sodium amalgam in THF affords the extremely air-sensitive one-electron reduction product which was crystallised as the  $[\text{Na}(15\text{-crown-5})_{1.5}]^+$  salt in 44% yield. Alternatively, the analogous  $\text{Cp}'$  complex has been prepared by the thermal decomposition of the thiolate adduct  $[\text{Mo}_2\text{Co}_2\text{S}_3\text{Cp}'_2(\text{CO})_2(\text{SAr})]^-$  ( $\text{Ar} = p\text{-tolyl}$ ) formed from  $[\text{Mo}_2\text{Co}_2\text{S}_3\text{Cp}'_2(\text{CO})_4]$  and  $p\text{-toluene thiolate}$  in acetonitrile. The addition of an electron causes an increase of ca. 0.4 Å in the Co–Co bond length with respect to the neutral 20 metal electron cluster, while the Mo–Mo and Mo–Co distances remain practically unchanged.<sup>[26]</sup> Thus, in a formal sense, changes in the number of metal electrons mainly involve the Co atoms; these are reduced from  $\text{Co}^{2+}$  to  $\text{Co}^{1.5+}$ .

Oxidation of the heterodimetallic sulfidocobalt cluster  $[\text{Mo}_2\text{Co}_2\text{S}_4\text{Cp}^{\text{Et}}_2(\text{CO})_2]$  with  $\text{X}_2$  ( $\text{X} = \text{Cl}, \text{Br}, \text{I}, \text{SPh}$ ) causes oxidative substitution of the carbonyl groups by halogens or  $\text{PhS}$  to give the 18 metal electron clusters  $[\text{Mo}_2\text{Co}_2\text{S}_4\text{Cp}^{\text{Et}}_2\text{X}_2]$  in 48–83% yields, as shown in Equation (2).<sup>[21,41]</sup>

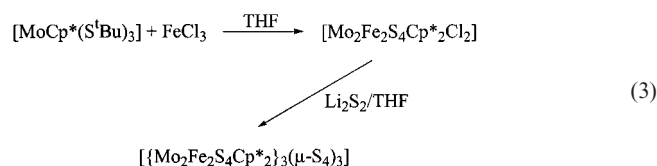


The  $\text{Mo}_2\text{Co}_2\text{S}_4$  core in these 18 electron metal clusters shows a cubane butterfly structure with five metal–metal bonds. The  $\text{Co}\cdots\text{Co}$  distances in these complexes are 2.934(3) and 2.953(3) Å for the iodine and the chlorine derivatives, respectively, and 2.741(1) Å for the thiolato cluster. This last value is very similar to that found for the radical anion  $[\text{Na}(15\text{-crown-5})_{1.5}][\text{Mo}_2\text{Co}_2\text{S}_4\text{Cp}^{\text{Et}}_2(\text{CO})_2]$  [2.735(1) Å] that was associated with a formal  $\text{Co}\cdots\text{Co}$  bond order of 1/2.

A (carbonyl) $\text{Mo}_2\text{Fe}_2\text{S}_4$  cubane-type cluster of formula  $[\text{Mo}_2\text{Fe}_2\text{S}_4\text{Cp}^{\text{Et}}_2(\text{CO})_4]$  has been synthesised from the molybdenum(IV) complex  $[\text{Mo}_2(\mu_2, \eta^2\text{-S}_2)(\mu_2\text{-S})_2\text{Cp}^{\text{Et}}_2]$ , by reaction with  $[\text{Fe}_2(\text{CO})_9]$  in THF at room temperature (33% yield) or by photochemical reaction with  $[\text{Fe}(\text{CO})_5]$  (10% yield).<sup>[30]</sup> Two heterodimetallic  $\text{Mo}_2\text{Fe}_2\text{S}_4$  trimers with a trigonal-bipyramidal core are also obtained from this reaction. The  $[\text{Mo}_2\text{Fe}_2\text{S}_4\text{Cp}^{\text{Et}}_2(\text{CO})_4]$  complex possesses 18 metal cluster electrons which agrees with a formal oxidation state assignment of  $\text{Mo}_2^{\text{IV}}\text{Fe}_2^{\text{II}}$ . The cubane cluster with 18 metal cluster electrons adopts a butterfly structure and consequently five metal–metal bonds. The coordination sphere around the iron atom consists of three  $\mu_3\text{-S}$  sulfur atoms and two carbonyl groups in a square-pyramidal geometry.

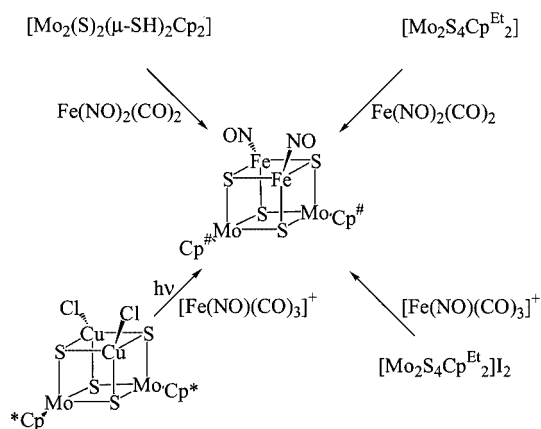
In the case of iron, the cyclopentadienyl halide derivative  $[\text{Mo}_2\text{Fe}_2\text{S}_4\text{Cp}^{\text{Et}}_2\text{Cl}_2]$  has been prepared through a self-assembly reaction between the molybdenum(IV) monomer

$[\text{MoCp}^*(\text{S}(t\text{Bu})_3)]$  and  $\text{FeCl}_3$  in THF that unexpectedly gives the cubane cluster  $[\text{Mo}_2\text{Fe}_2\text{S}_4\text{Cp}^{\text{Et}}_2\text{Cl}_2]$  in 39% yield.<sup>[20]</sup> The resulting  $[\text{Mo}_2\text{Fe}_2\text{S}_4]$  complex has 16 metal cluster electrons, and in spite of the uncertainty related to the oxidation state definition in cluster compounds, a possible assignment is  $\text{Mo}_3^{\text{IV}}\text{Fe}_2^{\text{II}}$ . The reduction of iron from  $\text{Fe}^{\text{III}}$  to  $\text{Fe}^{\text{II}}$  is considered to occur during the cluster formation reaction, with simultaneous cleavage of the C–S bond. The electron deficiency in this cluster mainly affects the Fe–Fe distance which is ca. 0.09 Å longer than in similar iron complexes having 20 metal electrons, as can be observed in Table 1. Reaction of  $[\text{Mo}_2\text{Fe}_2\text{S}_4\text{Cp}^{\text{Et}}_2\text{Cl}_2]$  with  $\text{Li}_2\text{S}_2$  gives rise to a tricubane cluster where the three  $\text{Mo}_2\text{Fe}_2\text{S}_4$  cluster units are linked by three Fe–Fe bonds (2.610 Å) and three  $\mu_2, \eta^2\text{-S}_4^{2-}$  ligands, as represented in Equation (3).



The only example of a heterodimetallic  $\text{Mo}_2\text{Cu}_2$  cluster with cyclopentadienyl ligands is the  $[\text{Mo}_2\text{Cu}_2\text{S}_4\text{Cp}^{\text{Et}}_2\text{Cl}_2]$  complex, prepared by reaction of  $[\text{Mo}_2\text{S}_4\text{Cp}^{\text{Et}}_2]$  with 2 equiv. of  $\text{CuCl}$  in acetonitrile. Three different isomeric forms of the dinuclear sulfido starting material have been used, namely  $[\text{Mo}_2(\mu_2, \eta^2\text{-S}_2)\text{S}_2\text{Cp}^{\text{Et}}_2]$ ,  $[\text{Mo}_2(\mu_2, \eta^2\text{-S}_2)(\mu_2\text{-S})_2\text{Cp}^{\text{Et}}_2]$ , and  $[\text{Mo}_2(\mu_2\text{-S})_2\text{S}_2\text{Cp}^{\text{Et}}_2]$ , and the best yields (81%) are obtained for the first of these. In all three cases, other trimetallic  $\text{Mo}_2\text{Cu}$  and noncuboidal tetrametallic  $\text{Mo}_2\text{Cu}_2$  complexes are also obtained as coproducts. The resulting  $[\text{Mo}_2\text{Cu}_2\text{S}_4\text{Cp}^{\text{Et}}_2\text{Cl}_2]$  complex having 22 metal electrons has a similar cubane-butterfly structure to the one observed for the 22 electron  $\text{Mo}_2\text{Ni}_2$  systems.<sup>[28]</sup>

Finally, several nitrosyl derivatives of the  $\text{M}_2\text{M}'_2\text{S}_4$  unit derived from (cyclopentadienyl)group-6 complexes have been prepared with Fe and Co as heterometals. These complexes have the chemical formula  $[\text{M}_2\text{M}'_2\text{S}_4\text{Cp}^{\text{Et}}_2(\text{NO})_2]$  ( $\text{M} = \text{Mo}$  and  $\text{W}$  and  $\text{M}' = \text{Fe}$  and  $\text{Co}$ ).<sup>[22,42]</sup> The clusters  $[\text{Mo}_2\text{Fe}_2\text{S}_4\text{Cp}^{\text{Et}}_2(\text{NO})_2]$  ( $\text{Cp}^{\text{Et}} = \text{Cp}, \text{Cp}^{\text{Et}}, \text{Cp}^*$ ) were synthesised using different Mo/S synthons and two (nitrosyl)Fe complexes as the source of the  $\text{FeNO}$  vertex, as summarised in Scheme 4. Typical yields for these reaction are ca. 40%. In contrast to the carbonylcobalt findings, the reaction between the (sulfhydryl)molybdenum complex  $[\text{Mo}_2\text{S}_2(\text{SH})_2\text{Cp}_2]$  and  $[\text{Fe}(\text{CO})_2(\text{NO})_2]$  does not lead to the “ $\text{Mo}_2\text{Fe}_2\text{S}_3$ ” cluster, isoelectronic with  $[\text{Mo}_2\text{Co}_2\text{S}_3\text{Cp}^{\text{Et}}_2(\text{CO})_2]$ .<sup>[22]</sup> It is interesting to point out that when the 22 electron cluster  $[\text{Mo}_2\text{Cu}_2\text{S}_4\text{Cp}^{\text{Et}}_2\text{Cl}_2]$  is irradiated in the presence of  $[\text{Fe}(\text{NO})(\text{CO})_3]^+$ , the  $\text{CuCl}$  fragments are replaced by  $\text{Fe}(\text{NO})$  to afford the 20 metal electron cluster  $[\text{Mo}_2\text{Fe}_2\text{S}_4\text{Cp}^{\text{Et}}_2(\text{NO})_2]$ .<sup>[28]</sup>



Scheme 4. Synthetic routes to the  $[\text{Mo}_2\text{Fe}_2\text{S}_4\text{Cp}^*(\text{NO})_2]$  cubane.

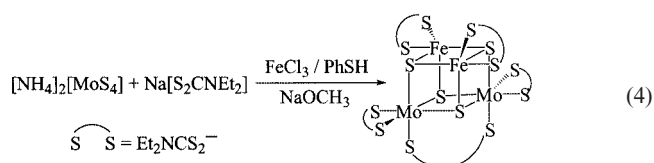
The analogous (nitrosyl) $\text{W}_2\text{Fe}_2$  complex is obtained by reaction of  $[\text{W}_2\text{S}_4\text{Cp}^*_2]$  with  $[\text{Fe}(\text{NO})_2(\text{CO})_2]$  in refluxing toluene to afford  $[\text{W}_2\text{Fe}_2\text{S}_4\text{Cp}^*_2(\text{NO})_2]$  in 36% yield. These  $[\text{M}_2\text{Fe}_2\text{S}_4\text{Cp}^*_2(\text{NO})_2]$  compounds have 20 metal cluster electrons and their structures show six metal–metal bonds and an NO ligand attached to the tetrahedral Fe atom. Similar cluster complexes are obtained for cobalt by treating  $[\text{Mo}_2\text{S}_4\text{Cp}^*_2]$ ,  $[\text{W}_2\text{S}_4\text{Cp}^*_2]$  or  $[\text{Mo}_2(\mu_2\text{-S})_2(\mu\text{-SH})_2\text{Cp}_2]$  with  $[\text{Co}(\text{CO})_3(\text{NO})]$  in toluene to afford complexes with formula  $[\text{M}_2\text{Co}_2\text{S}_4\text{Cp}^*_2(\text{NO})_2]$  in low to moderate (30–50%) yields.<sup>[22]</sup> The change of iron for cobalt increases the number of metal cluster electrons from 20 to 22. The formal oxidation states of the metal atoms in these clusters are  $\text{M}^{\text{III}}$  and  $\text{Co}^{\text{I}}$  (the nitrosyl ligand is assumed to be  $\text{NO}^+$ ) and consequently, replacement of Fe by Co has the same effect as substitution of a carbonyl by a nitrosyl group. The Co–Co distances of ca. 3.12 Å in the  $[\text{M}_2\text{Co}_2\text{S}_4\text{Cp}^*_2(\text{NO})_2]$  clusters (see Table 1) are well beyond the typical Co–Co single bond lengths and the metal atoms adopt the butterfly disposition already observed for other 22 metal electron clusters.

### $\text{M}_2\text{M}'_2\text{S}_4$ Clusters with Sulfur-Containing Ligands

The number of  $\text{M}_2\text{M}'_2$  clusters with sulfur-containing ligands is more limited than their cyclopentadienyl counterparts. All known examples contain dithiolate or dithiocarbamate as ancillary ligands and metal electron counts between 15 and 20. The main building block fragment used for this chemistry is the *syn*- $[\text{M}_2(\mu_2\text{-S})_2\text{S}_2]$  unit, in particular the molybdenum and tungsten dimers  $[\text{M}_2\text{S}_4(\text{dte})_2]$  (dte = diethyldithiocarbamate) and  $[\text{Et}_4\text{N}]_2[\text{M}_2\text{S}_4(\text{edt})_2]$  (edt = 1,2-ethanedithiolate). The *syn* isomers of the molybdenum complexes  $[\text{Mo}_2(\mu_2\text{-S})_2\text{S}_2(\text{dte})_2]$  and  $[\text{Mo}_2(\mu_2\text{-S})_2\text{S}_2(\text{edt})_2]^{2-}$  are prepared in 82 and 75% yield, respectively, by reaction of  $[\text{NH}_4]_2[\text{Mo}_2(\text{S-S})_6]$  with an excess (20–25 equiv.) of Na[dte] or  $\text{Na}_2[\text{edt}]$  in refluxing methanol.<sup>[43]</sup> The excess thiolate serves both as the reductant of the disulfide ligand and as a peripheral ligand in the final product. The necessity for excess thiolate may be obviated by using triphenyl-

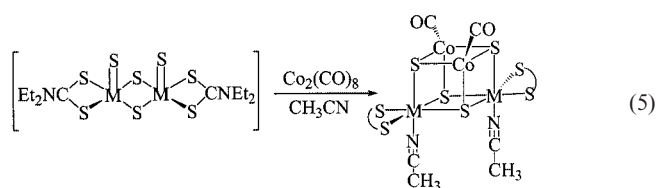
phosphane as the reducing agent. A more general route for the synthesis of  $[\text{Et}_4\text{N}]_2[\text{Mo}_2(\mu_2\text{-S})_2\text{S}_2(\text{edt})_2]$  has been developed, and this can also be used to prepare the analogous tungsten complex.  $[\text{NH}_4]_2[\text{MS}_4]$  is treated with 1,3-ethanedithiol in DMF, and addition of tetraethylammonium bromide precipitates the  $[\text{Et}_4\text{N}]_2[\text{M}_2(\mu_2\text{-S})_2\text{S}_2(\text{edt})_2]$  salt in 63 and 55% yields for Mo and W respectively.<sup>[44,45]</sup> The tungsten complex  $[\text{W}_2(\mu_2\text{-S})_2\text{S}_2(\text{dte})_2]$  can be obtained in 75% yield by treatment of  $(\text{Et}_4\text{N})_2[\text{W}_2(\mu_2\text{-S})_2\text{S}_2(\text{S}_4)]$  with sodium diethyldithiocarbamate, triphenylphosphane and  $\text{NH}_4\text{PF}_6$  in acetonitrile.<sup>[45]</sup> The sulfur-rich  $[\text{W}_2(\mu_2\text{-S})_2\text{S}_2(\text{S}_4)_2]^{2-}$  anion has also been employed as a building block. This tungsten(v) dimer is obtained in 83% yield by heating  $[\text{NH}_4]_2[\text{WS}_4]$  and elemental sulfur in DMF.<sup>[45]</sup> It can also be obtained at room temperature by using a reducing agent such as  $\text{NH}_2\text{NH}_2\cdot\text{HCl}$ .<sup>[32]</sup>

The synthesis of the cubane cluster  $[\text{Mo}_2\text{Fe}_2\text{S}_4(\text{S}_2\text{CNET}_2)_5]$  in 18% yield has been reported, using a one-pot reaction between  $[\text{NH}_4]_2[\text{MoS}_4]$ ,  $\text{FeCl}_3$ ,  $\text{Na}[\text{dte}]$ ,  $\text{PhSH}$  and  $\text{NaOCH}_3$  in methanol/DMF solutions, as shown in Equation (4).<sup>[29]</sup>

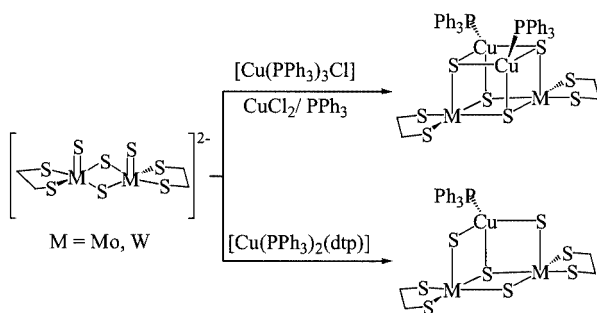


It is very likely that the reducing conditions used in this reaction ( $\text{PhS}^-$  and  $\text{Et}_2\text{NCS}_2^-$ ) cause the formation of an intermediate molybdenum(v) dimer with an  $\text{M}_2(\mu_2\text{-S})_2\text{S}_2$  central core, as found for tungsten. The  $\text{Mo}_2\text{Fe}_2\text{S}_4$  cluster skeleton has a cubane-type structure where each metal atom is coordinated by three  $\mu_3\text{-S}$  atoms and two sulfur atoms of the dithiocarbamate chelating terminal ligand. In addition, the fifth  $\text{Et}_2\text{NCS}_2^-$  group acts as a bridging ligand between two Mo atoms, resulting in an octahedral environment for that metal atom. The coordination geometry around the iron atom is an irregular triangular bipyramid. The intermetallic distances within this cluster are listed in Table 1. The Mo–Mo and Mo–Fe bond lengths are consistent with metal–metal single bonds, while the Fe–Fe bond length of 2.784 Å lies outside the single bond range. In consequence there are in total five metal–metal bonds, with the metal atoms defining a butterfly arrangement in which the Mo atoms occupy the hinge positions. The dithiocarbamate bridging ligand causes a shortening of the Mo–Mo bond length (2.734 Å) in the  $[\text{Mo}_2\text{Fe}_2\text{S}_4(\text{S}_2\text{CNET}_2)_5]$  cluster, while the other intermetallic Mo–Fe and Fe–Fe bond lengths are similar to those observed in the 16 metal electron cluster  $[\text{Mo}_2\text{Fe}_2\text{S}_4\text{Cp}^*_2\text{Cl}_2]$ .

The  $\text{Mo}_2\text{Co}_2\text{S}_4$  cluster  $[\text{Mo}_2\text{Co}_2\text{S}_4(\text{S}_2\text{CNET}_2)_2(\text{CH}_3\text{CN})_2(\text{CO})_2]$  having 20 metal cluster electrons has been prepared by reaction of  $[\text{Mo}_2(\mu_2\text{-S})_2\text{S}_2(\text{dte})_2]$  with an equimolar amount of  $[\text{Co}_2(\text{CO})_8]$  in THF or acetonitrile, as represented in Equation (5).<sup>[23]</sup>



The analogous tungsten complex is prepared from  $[\text{W}_2(\mu_2\text{-S})_2\text{S}_2(\text{dtc})_2]$  in acetonitrile.<sup>[45]</sup> The structure of the parent  $[\text{M}_2\text{S}_4(\text{dtc})_2]$  fragment remains essentially unchanged in the final cluster, where the  $\text{M}_2\text{Co}_2$  atoms define a tetrahedron. The dinuclear precursor shows no tendency to bind acetonitrile, in contrast to the final cubane product, and thus it appears that the presence of cobalt enhances the affinity for ligands at the molybdenum or tungsten site *trans* to the  $\mu_3\text{-S}$  atom. There are no known examples of  $\text{M}_2\text{Ni}_2\text{S}_4$  derivatives with sulfur-containing ligands and examples with copper are restricted to the molybdenum and tungsten  $[\text{M}_2\text{Cu}_2\text{S}_4(\text{SCH}_2\text{CH}_2\text{S})_2(\text{PPh}_3)_2]$  complexes. When  $[\text{Et}_4\text{N}]_2[\text{MoS}_4(\text{edt})_2]$  reacts with 2 equiv. of  $[\text{Cu}(\text{PPh}_3)_3\text{Cl}]$  under an inert gas, the cubane cluster compound  $[\text{Mo}_2\text{Cu}_2\text{S}_4(\text{edt})_2(\text{PPh}_3)_2]$  is obtained. The isomorphous tungsten compound  $[\text{W}_2\text{Cu}_2\text{S}_4(\text{edt})_2(\text{PPh}_3)_2]$  was synthesised from  $[\text{Et}_4\text{N}]_2[\text{WS}_4(\text{edt})_2]$ ,  $\text{CuCl}_2\cdot\text{H}_2\text{O}$  and  $\text{PPh}_3$  in  $\text{CH}_2\text{Cl}_2/\text{EtOH}$  solution.<sup>[31]</sup> The coordination sphere around the Mo or W atoms in these complexes consists of three  $\mu_3\text{-S}$  sulfido ligands and two sulfur atoms from the bidentate ligand, arranged in a tetragonal-pyramidal geometry. The four metal atoms adopt a cubane-butterfly structure, as found in the (cyclopentadienyl) $\text{M}_2\text{Cu}_2$  derivatives which also have 22 metal cluster electrons.<sup>[33]</sup> Alternatively, the reaction of  $[\text{Et}_4\text{N}]_2[\text{M}_2\text{S}_4(\text{edt})_2]$  ( $\text{M} = \text{Mo}, \text{W}$ ) with  $[\text{Cu}(\text{PPh}_3)_2(\text{dtp})]$  ( $\text{dtp} = ^-\text{S}_2\text{P}(\text{OCH}_2\text{-CH}_3)_2$ , dithiophosphate) in  $\text{CH}_2\text{Cl}_2/\text{CH}_3\text{CN}$  solution at room temperature gives the incomplete cubane cluster  $[\text{Et}_4\text{N}][\text{M}_2\text{CuS}_4(\text{edt})_2(\text{PPh}_3)]$  ( $\text{M} = \text{Mo}, \text{W}$ ), as summarised in Scheme 5.<sup>[46]</sup>



Scheme 5. Incorporation of one or two copper atoms to  $(\text{Et}_4\text{N})_2[\text{M}_2\text{S}_2(\mu_2\text{-S})_2(\text{edt})_2]$

No interconversion between the trinuclear and the tetranuclear species, as has been found in similar systems with noble metals instead of copper, has been reported.<sup>[47]</sup>

Finally, the air-stable complex  $[\text{Et}_4\text{N}]_4[\text{W}_2\text{Cu}_2\text{S}_4(\text{SCN})_8]$  having 22 metal cluster electrons has been prepared in 45% yield by reacting  $[\text{Et}_4\text{N}]_2[\text{W}_2\text{S}_4(\text{S}_4)_2]$  with  $\text{CuCl}$  in the presence of  $\text{KSCN}$ .<sup>[32]</sup> In contrast to the other complexes described in this section, the tungsten atom is coordinated to the nitrogen atoms of the thiocyanate ligands in a octahedral coordination environment. The thiocyanate ligands attached to the Cu atoms define a tetrahedron. All the reported  $\text{M}_2\text{Cu}_2\text{S}_4$  clusters are electron-precise, having 22 metal cluster electrons (see Table 1) and a cuboidal–butterfly arrangement of the metal atoms, where the nonbonding distance corresponds to the  $\text{Cu}\cdots\text{Cu}$  interaction.

### Clusters with $\text{M}_3\text{M}'\text{Q}_4$ Central Units

In contrast to the above-reported cuboidal complexes where, with the exception of the  $[\{\text{Mo}_2\text{Fe}_2\text{S}_4\text{Cp}^*_{2}\}_3(\mu\text{-S}_4)_3]$  tricubane cluster, only isolated single-cube structures have been found, compounds with  $\text{M}_3\text{M}'\text{Q}_4$  central cores exhibit single, edge linked double-cube and corner-shared double-cube structures, as represented in Figure 2. In the case of first-row transition heterometals, only the first two structural types have been encountered to date.

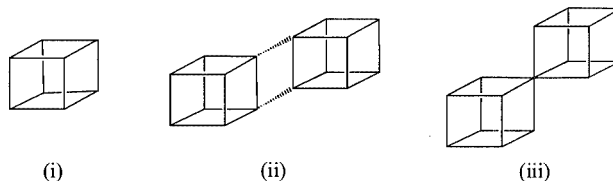


Figure 2. Structural types of  $\text{M}_3\text{M}'\text{Q}_4$  aquo cuboidal clusters: (i) single cubane (ii) edge-linked double cubane (iii) corner-shared double cubane

The chemistry of heterodimetallic clusters with  $\text{M}_3\text{M}'\text{Q}_4$  cores has been developed predominantly in aqueous media, and major advances have been made in the field of molybdenum clusters, where the heterometals incorporated into the incomplete cuboidal  $[\text{Mo}_3\text{S}_4(\text{H}_2\text{O})_9]^{4+}$  aquo ion according to a  $[3 + 1]$  synthetic strategy range from group-6 to -15 elements.<sup>[18]</sup> For tungsten, the number of heterometals incorporated is more restricted, a fact that has been attributed to the greater difficulty in reducing tungsten as compared to molybdenum. Reactivity studies of  $[\text{M}_3\text{Se}_4(\text{H}_2\text{O})_9]^{4+}$  complexes towards a second metal are limited to some preliminary results regarding the incorporation of Ni and Pd into the molybdenum selenide aquo ion<sup>[48]</sup> and Mo insertion into the  $\text{W}_3\text{Se}_4$  aquo ion.<sup>[49]</sup> This chemistry has been extensively reviewed in the past year, and for this reason we will only comment on the most relevant aspects regarding the insertion of first-row transition metals into the  $\text{M}_3\text{Q}_4$  aquo ion. However, we will give a detailed description of the non-aqueous chemistry of these  $\text{M}_3\text{M}'\text{Q}_4$  heterodimetallic clusters.<sup>[17–19]</sup> Figure 3 presents a number of representative  $\text{M}_3\text{M}'\text{Q}_4$  clusters that have been

reported, where again the familiar cubane core has been emphasised.

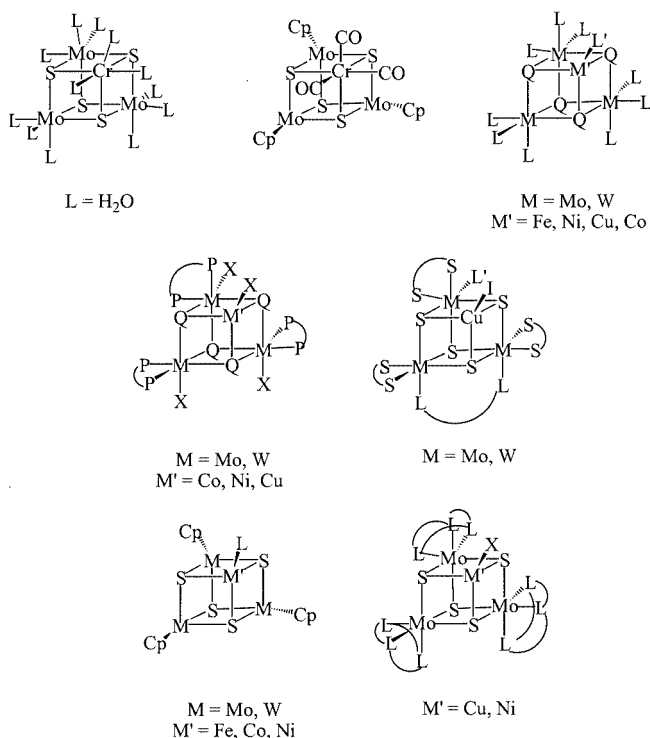


Figure 3. Schematic representations of cubane structures and metal environments of  $M_3M'Q_4$  clusters

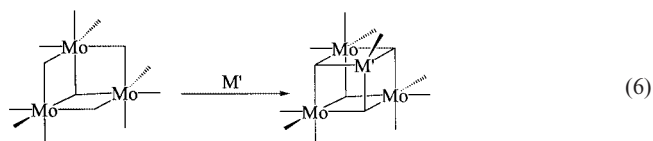
### $M_3M'Q_4$ Clusters as Derivatives of the $M_3Q_4$ Aquo Ion

Since Shibahara's report in 1986 of the reaction of the molybdenum aquo cluster  $[Mo_3S_4(H_2O)_9]^{4+}$  with iron metal to give the molybdenum–iron mixed-metal cluster  $[Mo_3FeS_4(H_2O)_{10}]^{4+}$ , much work has been carried out in the field.<sup>[50]</sup> The insertion of other metal atoms has been successfully achieved as previously mentioned, and the analogous tungsten and selenium building blocks  $M_3Q_4$  have been prepared.

The synthesis of the green aquo cluster  $[Mo_3S_4(H_2O)_9]^{4+}$  has been recently reviewed.<sup>[17]</sup> This aquo ion was first prepared in low yields (ca. 20%) by two different routes; the self-assembly reaction of  $[Mo(CO)_6]$  with anhydrous  $Na_2S$  in acetic anhydride<sup>[51]</sup> and oxidative fragmentation of the tetrametallic  $[Mo_4S_4(H_2O)_{12}]^{5+}$  aquo ion in acidic solutions.<sup>[52,53]</sup> An almost quantitative synthesis of this aquo ion has been developed that involves abstraction of sulfur from the  $[Mo_3(\mu_3-S)(\mu_2-S_2)_3X_6]^{2-}$  ( $X = Cl, Br$ ) trimer with  $PPh_3$ .<sup>[54]</sup> The analogous selenium cluster  $[Mo_3Se_4(H_2O)_9]^{4+}$  has been prepared in a similar manner from the selenium-rich trimer  $[PPh_4]_2[Mo_3(\mu_3-Se)(\mu_2-Se_2)_3Cl_6]$ , which was aquated in acid prior to the diselenide reduction to selenide with  $PPh_3$ .<sup>[55]</sup> The most efficient method for the synthesis of the  $[W_3Q_4(H_2O)_9]^{4+}$  aquo ions (yields ca. 60–70%) involves treatment of the corresponding  $\{W_3Q_7Br_4\}_x$  polymeric phases with hypophosphorous acid in hot HCl.<sup>[56,57]</sup> Purification of the aquo ions is achieved by cation exchange

chromatography. The sulfur-bridged trimers are stable in acidic solution, but the selenium analogues are less stable, giving a deposit of red selenium after a week.<sup>[57,58]</sup>

First-row transition metal incorporation into the  $[Mo_3S_4]^{4+}$  aquo ion has been achieved by treating  $[Mo_3S_4(H_2O)_9]^{4+}$  with iron,<sup>[50]</sup> cobalt,<sup>[59]</sup> nickel<sup>[60]</sup> and copper metal<sup>[61]</sup> ( $M'$ ) in acidic solution, HCl or *p*-toluenesulfonic acid (Hpts), to afford the corresponding heterodimetallic  $[Mo_3M'S_4(H_2O)_{10}]^{4+}$  complexes with 14, 15, 16 and 17 metal cluster electrons for  $M' = Fe, Co, Ni$  and  $Cu$ , respectively, as shown in Equation (6).



This synthetic strategy has also been applied to obtain the selenido derivative  $[Mo_3NiSe_4(H_2O)_{10}]^{4+}$ <sup>[48]</sup> or the tungsten-containing cluster sulfides  $[Mo_{3-x}W_xNiS_4(H_2O)_{10}]^{4+}$  ( $x = 0-3$ ).<sup>[62]</sup> Alternatively, the  $[Mo_3NiS_4(H_2O)_{10}]^{4+}$  aquo ion has been synthesised by a self-assembly reaction between  $[NH_4]_2[MoS_4]$  and nickel metal in HCl solution or by reduction of an  $Ni^{2+}$  salt in the presence of  $[Mo_3S_4(H_2O)_9]^{4+}$ .<sup>[63,64]</sup> With the exception of the  $[Mo_3NiS_4(H_2O)_{10}]^{4+}$  complex, the remaining heterodimetallic aquo ions, especially the cobalt derivative, are very air-sensitive.

The  $Mo_3Fe$  and  $Mo_3Ni$  aquo ions, having an even number of cluster metal electrons, crystallised from *p*-toluenesulfonic acid solutions as isolated single cubes of formula  $[Mo_3M'S_4(H_2O)_{10}](pts)_4 \cdot 7H_2O$  ( $pts = p$ -toluenesulfonate), while the analogous Co and Cu heterodimetallic clusters, having an odd number of metal electrons, crystallise under the same conditions as an edge-linked double cuboidal structure formulated as  $\{[Mo_3M'S_4(H_2O)_9]_2(pts)_8 \cdot nH_2O\}$  ( $M' = Co, n = 18$ ;  $M' = Cu, n = 20$ ). The Co–Co and Cu–Cu bond lengths in these double cubes are 2.498 and 2.426 Å, respectively, corresponding to an  $M'-M'$  single bond. A summary of intermetallic distances for  $M_3M'S_4$  cubanes is presented in Table 2.

In contrast to the  $[M_2M'_2S_4]$  heterodimetallic complexes, changes in the heterometal within the  $[Mo_3M'S_4]^{4+}$  aquo ion series does not produce significant differences in the intermetallic distances that can be correlated with the number of metal cluster electrons. The single-to-double cube dimerisation reaction is reversible in the case of Cu, as shown in Equation (7).<sup>[76,77]</sup>

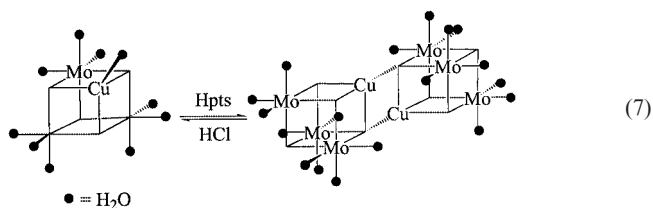




Table 2. Selected bond lengths [ $\text{\AA}$ ] for some representative  $\text{M}_3\text{M}'\text{S}_4$  cubane-type clusters (standard deviations for averaged values are given in brackets)

Cluster	No. of metal electrons	M–M	M–M'	Ref.
Single cubes:				
$[\text{Mo}_3\text{FeS}_4(\text{H}_2\text{O})_{10}]^{4+}$	14	2.767[7]	2.671[11]	[65]
$[\text{Mo}_3\text{FeS}_4\text{Cp}'_3(\text{SH})]$	14	2.86[2]	2.79[2]	[24]
$[\text{Mo}_3\text{CoS}_4\text{Cp}'_3\text{CO}]$	16	2.838[11]	2.745[11]	[24]
$[\text{Mo}_3\text{NiS}_4(\text{H}_2\text{O})_{10}]^{4+}$	16	2.755[10]	2.640[9]	[60]
$[\text{Mo}_3\text{NiS}_4(\text{H}_2\text{O})_9\text{CO}]^{4+}$	16	2.744[8]	2.677[7]	[66]
$[\{\text{Mo}_3\text{NiS}_4\text{Cp}'_3\}_2(\mu\text{-C}_4\text{H}_8\text{S}_2)]^{2+}$	16	2.819[13]	2.71[1]	[67]
$[\text{W}_3\text{NiS}_4(\text{H}_2\text{O})_9(\text{C}_2\text{H}_4)]^{4+}$	16	2.7137(9)	2.701(2)	[62]
$[\text{W}_3\text{NiS}_4\text{Cp}'_3(\text{PPh}_3)]^+$	16	2.809[1]	2.733[9]	[68]
$[\text{Mo}_3\text{CuS}_4(\text{Hnta})_3\text{Cl}]^{2-}$	16	2.778(1)	2.838(2)	[69]
$[\text{Mo}_3\text{CuS}_4(\text{dmpe})_3\text{Cl}_4]^+$	16	2.782[1]	2.823[8]	[5]
$[\text{W}_3\text{CuS}_4(\text{dmpe})_3\text{Br}_4]^+$	16	2.780[2]	2.884[7]	[5]
$[\text{Mo}_3\text{CuS}_4(\text{dtp})_3(\mu\text{-OAc})(\text{DMF})\text{I}]$	16	2.73[5]	2.85[4]	[70]
$[\text{Mo}_3\text{CuS}_4(n\text{Pr}_2\text{PS}_2)_3(\mu\text{-}n\text{Pr}_2\text{PS}_2)(\text{py})\text{I}]$	16	2.769[9]	2.857[14]	[71]
$[\text{W}_3\text{CuS}_4(\text{dtp})_3(\mu\text{-O}_2\text{CCl}_3)(\text{CH}_3\text{CN})\text{I}]$	16	2.73[3]	2.87[5]	[72]
$[\text{Mo}_3\text{CuS}_4(\text{Et}_2\text{NCS}_2)_3(\mu\text{-Et}_2\text{NCS}_2)(\text{py})\text{I}]$	16	2.76[3]	2.849[13]	[73]
$[\text{Mo}_3\text{CuS}_4(\text{tdci})_3\text{Br}]^{3+}$	17	2.832[9]	2.916[12]	[74]
$[\text{Mo}_3\text{CuSe}_4(\text{dmpe})_3\text{Cl}_4]^+$	16	2.839[4]	2.839[4]	[75]
Edge-linked double cubes:				
$[\{\text{Mo}_3\text{CoS}_4(\text{H}_2\text{O})_9\}_2]^{8+}$	15	2.744[11]	2.64[2]	[59]
$[\{\text{W}_3\text{NiS}_4(\text{H}_2\text{O})_9\}_2]^{8+}$	16	2.747[7]	2.66[4]	[62]
$[\{\text{Mo}_3\text{CuS}_4(\text{H}_2\text{O})_9\}_2]^{8+}$	17	2.730[7]	2.89[8]	[61]

The  $[\text{Mo}_2\text{W}\text{Ni}]^{4+}$  aquo ions crystallise as single cuboidal clusters in the same way as the analogous  $\text{Mo}_3\text{Ni}$  complexes. However, further substitution of Mo for W results in the formation of  $[\{\text{Mo}_n\text{W}_{3-n}\text{NiS}_4(\text{H}_2\text{O})_9\}_2](\text{pts})_8 \cdot 20\text{H}_2\text{O}$  ( $n = 0, 1$ ) edge-linked double cuboidal structures, with Ni–Ni bond lengths of 2.549  $\text{\AA}$  for  $\text{MoW}_2\text{Ni}$  and 2.56  $\text{\AA}$  for the  $\text{W}_3\text{Ni}$  cluster.<sup>[62]</sup>

In contrast to the reactivity just reported for the incomplete cuboidal molybdenum sulfide versus a first-row transition metal, the  $[\text{Mo}_3\text{S}_4]^{4+}$  aquo ion does not react with chromium metal. Instead, the  $[\text{Mo}_3\text{CrS}_4(\text{H}_2\text{O})_{12}]^{4+}$  cluster is prepared by treating  $[\text{Mo}_3\text{S}_4(\text{H}_2\text{O})_9]^{4+}$  with  $[\text{Cr}(\text{H}_2\text{O})_6]^{2+}$ . This  $\text{Mo}_3\text{Cr}$  cube has only been characterised spectroscopically in solution.<sup>[78]</sup> The reaction of the  $[\text{Mo}_3\text{S}_4]^{4+}$  aquo ion with  $\text{Cu}^+$ , or with a  $\text{Cu}^{2+}$  salt in the presence of sodium borohydride, gives the 16 electron metal cluster  $[\text{Mo}_3\text{CuS}_4(\text{H}_2\text{O})_{10}]^{5+}$  in contrast to the 17 electron species obtained by direct reaction between the trimer and the metal.<sup>[76]</sup> The 16 electron  $\text{Mo}_3\text{Cu}$  clusters are air-stable in HCl due to coordination of  $\text{Cl}^-$  to the heterometal, but they tend to disproportionate to  $\text{Cu}^{2+}(\text{aq.})$  and  $[\text{Mo}_3\text{CuS}_4]^{4+}$  in noncoordinating acids.<sup>[69]</sup> The existence of the 16 metal electron  $[\text{Mo}_3\text{CuS}_4]^{5+}$  complex is also detected as the first step of the oxidation reaction of the corresponding 17 metal electron cluster.<sup>[76]</sup> The transmetallation reaction of  $[\text{Mo}_3\text{M}'\text{S}_4(\text{H}_2\text{O})_{10}]^{4+}$  ( $\text{M}' = \text{Fe}, \text{Ni}$ ) in the presence of a 10 molar excess of a  $\text{Cu}^{2+}$  salt in 2 M HCl also produces the 16 electron  $[\text{Mo}_3\text{CuS}_4(\text{H}_2\text{O})_9\text{Cl}]^{3+}$  aquo complex as the major reaction product.<sup>[79]</sup> When the cluster concentration is increased to ca. 0.1 M, the reaction of  $[\text{Mo}_3\text{FeS}_4(\text{H}_2\text{O})_{10}]^{4+}$  with a  $\text{Cu}^{2+}$  salt under similar conditions instead affords the 17 electron cluster

$[\text{Mo}_3\text{CuS}_4(\text{H}_2\text{O})_9\text{Cl}]^{4+}$  as the major product (yield = 37%), while the 16 electron cluster is only obtained in 5% yield.<sup>[69]</sup> Further investigations are required to understand these replacement reactions.

In the same way that chlorine coordination to the heteroatom stabilises the  $[\text{Mo}_3\text{CuS}_4]^{4+}$  cluster core, substitution of the water molecule coordinated to the extremely air-sensitive  $[\text{Mo}_3\text{CoS}_4]^{4+}$  aquo ion affords the more stable  $[\text{Mo}_3\text{CoS}_4(\text{H}_2\text{O})_9(\text{CO})]^{4+}$  cluster.<sup>[48]</sup> The nickel aquo cluster also coordinates CO and ethylene (L) in aqueous or organic solutions to give  $[\text{M}_3\text{NiS}_4(\text{H}_2\text{O})_9\text{L}]^{4+}$  and  $[\text{Mo}_3\text{NiSe}_4(\text{H}_2\text{O})_9\text{L}]^{4+}$ .<sup>[62]</sup> Coordination of ethylene is favoured by an increase in the number of tungsten atoms in the cluster core.

The heterodimetallic  $[\text{M}_3\text{M}'\text{S}_4]^{4+}$  cluster aquo ions can also be derivatised by substitution of the water molecules coordinated to the group-6 metal by mono-,<sup>[65]</sup> bi-<sup>[80]</sup> or tridentate ligands.<sup>[60]</sup> In some cases, this substitution results in complexes having an enhanced stability, a fact that has allowed the crystallisation and further X-ray characterisation of certain cluster cores. For example, addition of nitrilotriacetate ( $\text{H}_3\text{nta} + \text{base}$ ) to the  $[\text{Mo}_3\text{CuS}_4(\text{H}_2\text{O})_9\text{Cl}]^{4+}$  aquo complex allows crystallisation of the single cube  $[\text{Mo}_3\text{CuS}_4(\text{Hnta})_3\text{Cl}]^{2-}$  as the  $\text{K}^+$  or  $[\text{NH}_4]^+$  salt.<sup>[69]</sup> The Mo–Mo and Mo–Cu distances in this 16 metal electron cluster are similar to those observed for the  $[\{\text{Mo}_3\text{CuS}_4(\text{H}_2\text{O})_9\}_2](\text{pts})_8 \cdot 20\text{H}_2\text{O}$  double cube with 17 metal electrons per cubane unit. In other cases, derivatisation of the heterodimetallic  $[\text{M}_3\text{M}'\text{S}_4]^{4+}$  cluster aquo ions produces unexpected results. For example, reaction of  $[\text{Mo}_3\text{CuS}_4(\text{H}_2\text{O})_{10}]^{4+}$  with concentrated ammonia yields the  $[\{(\text{NH}_3)_6(\text{H}_2\text{O})(\text{OH})\text{Mo}_3\text{CuS}_4(\mu_2\text{-O})\}_2]\text{Cl}_4 \cdot 8\text{H}_2\text{O}$  com-

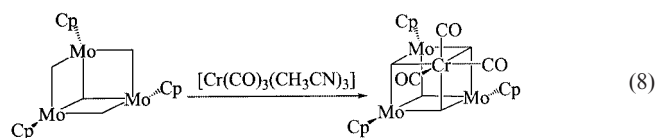
plex in which two cuboidal  $[\text{Mo}_3\text{CuS}_4]^{5+}$  cores are bridged by two oxygen atoms. The oxidant of the cluster core in this reaction remains unidentified.<sup>[81]</sup>

### $\text{M}_3\text{M}'\text{S}_4$ Clusters with Cyclopentadienyl Ligands

$[\text{Mo}_3\text{M}'\text{S}_4\text{Cp}_3]^{n+}$  ( $n = 0, 1$ ) cluster compounds with  $\text{M}' = \text{Cr}, \text{Fe}, \text{Co}$  and  $\text{Ni}$  have been prepared through  $[3 + 1]$  building-block synthetic strategies using the  $[\text{Mo}_3\text{S}_4\text{Cp}_3]^+$  incomplete cuboidal cluster as the precursor in the case of  $\text{Cr}$  and  $\text{Ni}$ , or by rearrangement of tetrametallic cluster species with  $\text{Mo}_2\text{Fe}_2$  and  $\text{Mo}_2\text{Co}_2$  units. Of the analogous tungsten complexes, only the nickel derivative  $[\text{W}_3\text{NiS}_4\text{Cp}'_3]^+$  has been prepared.

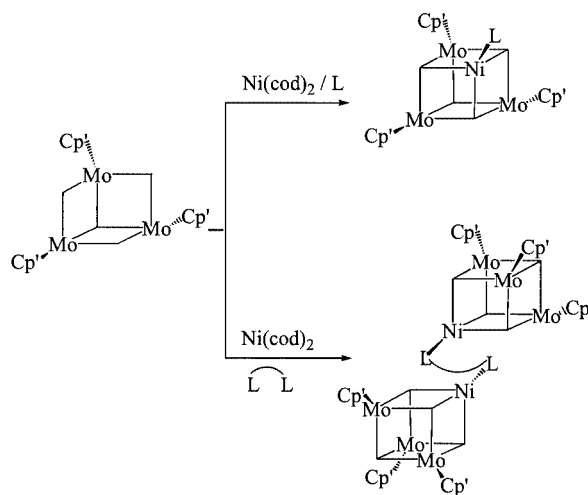
The synthesis of the trinuclear complex  $[\text{Mo}_3\text{S}_4\text{Cp}_3][\text{Sn}(\text{CH}_3)_3\text{Cl}_2]$  was first reported in 1971 from the reaction of  $[\text{MoCp}(\text{CO})_3\text{Cl}]$  with  $[\text{Sn}(\text{CH}_3)_3]_2\text{S}$  in 1,2-dimethoxyethane in 50% yield.<sup>[82]</sup> An improved synthetic procedure for this trimer that uses the  $[\text{Mo}_3\text{S}_4]^{4+}$  aquo ion as the starting material has recently been reported. This synthesis can also be used to prepare the analogous tungsten complex. Reaction of the  $[\text{M}_3\text{S}_4(\text{H}_2\text{O})_9]^{4+}$  ion ( $\text{M} = \text{Mo}$  or  $\text{W}$ ) with triethyl orthoformate in the presence of a catalytic amount of *p*-toluenesulfonic acid converts the aquo ligands into ethanol ligands which can be further replaced by acetonitrile and tetrahydrofuran. Finally, addition of  $\text{TiCp}$  or  $\text{TiCp}'$  results in formation of the desired  $[\text{M}_3\text{S}_4\text{Cp}^\#](\text{pts})$  ( $\text{Cp}^\# = \text{Cp}$  or  $\text{Cp}'$ ) species. Treatment with  $\text{CH}_3\text{CN}$  prior to THF is carried out to ensure removal of traces of  $(\text{CH}_3\text{CH}_2\text{O})_3\text{CH}$  and results in an improvement of the final yield. Typical yields for these reactions are 85% for molybdenum and 22% for tungsten.<sup>[68,83,84]</sup> The reduced  $[\text{Mo}_3\text{S}_4\text{Cp}^\#]$  ( $\text{Cp}^\# = \text{Cp}, \text{Cp}^*$ ) species have been synthesised by reaction of  $[\text{MoH}(\text{CO})_3\text{Cp}]$  or  $[\text{MoH}(\text{CO})_2\text{Cp}[\text{P}(\text{OC}_6\text{H}_5)_3]]$  with propylene sulfide in THF or by reduction of  $[\text{Mo}\{\text{S}(\text{tBu})_3\}\text{Cp}^*]$  with sodium amalgam in 88% yield.<sup>[85,86]</sup>

$[\text{Mo}_3\text{S}_4\text{Cp}_3](\text{pts})$  reacts with  $[\text{Cr}(\text{CO})_3(\text{CH}_3\text{CN})_3]$  in  $\text{CH}_2\text{Cl}_2$  to produce  $[\text{Mo}_3\text{CrS}_4\text{Cp}_3(\text{CO})_3](\text{pts})$  in 64% yield, as represented in Equation (8).<sup>[83]</sup>



This  $\text{Mo}_3\text{CrS}_4$  cluster is stable in air for at least a few days and soluble in common polar organic solvents. This reaction also works for the analogous molybdenum and tungsten carbonylmetal compounds, showing that the  $[3 + 1]$  insertion reactions are not restricted to aqueous media. A nickel atom can also be incorporated into the  $[\text{Mo}_3\text{S}_4\text{Cp}'_3](\text{pts})$  and  $[\text{W}_3\text{S}_4\text{Cp}'_3](\text{pts})$  complexes by treating these trimeric precursors with  $[\text{Ni}(\text{cod})_2]$  ( $\text{cod} = 1,5$ -cyclooctadiene) to yield the coordinatively unsaturated cubane-like cluster  $[\text{M}_3\text{NiS}_4\text{Cp}'_3](\text{pts})$  in high yields.<sup>[68,87]</sup> The reac-

tion produces an instant colour change from green to dark brown in the case of molybdenum while, for the tungsten complex, the colour change from violet to brown takes approximately 3 h, probably due to solubility problems. Addition of various ligands to the reaction mixture [triphenylphosphane,  $\text{M} = \text{W}$ ; dimethyl sulfide, diethyl sulfide, di(*tert*-butyl) sulfide, tetrahydrothiophene, 1,4-dithiane, thiochroman-4-ol, pyridine, quinoline, 4,4'-bipyridine,  $\text{M} = \text{Mo}$ ] saturates the vacant Ni coordination site, as represented in Scheme 6.<sup>[67]</sup>



Scheme 6. Coordination of mono- and bidentate ligands to the  $[\text{Mo}_3\text{NiS}_4\text{Cp}'_3]^+$  cluster

The crystal structures of the tungsten derivative  $[\text{W}_3\text{NiS}_4\text{Cp}'_3(\text{PPh}_3)](\text{pts})$  and the molybdenum derivatives  $\{[\text{Mo}_3\text{NiS}_4\text{Cp}'_3]_2(\mu_2\text{-C}_4\text{H}_8\text{S}_2)](\text{pts})_2$  and  $\{[\text{Mo}_3\text{NiS}_4\text{Cp}'_3]_2(\mu_2\text{-(4,4'-bipy)})](\text{pts})_2$  have been determined. In the last two examples, the 1,4-dithiane and the 4,4'-bipyridine ligands act as bridges between two cubane units. The intermetallic distances for these  $\text{M}_3\text{Ni}$  complexes having 16 metal electrons are similar to those found for the analogous aquo derivatives (see Table 2). Structural data for the molybdenum complexes, where the Ni atom coordinates a sulfur or a nitrogen atom, do not indicate any activation of the C–S or C–N bond.

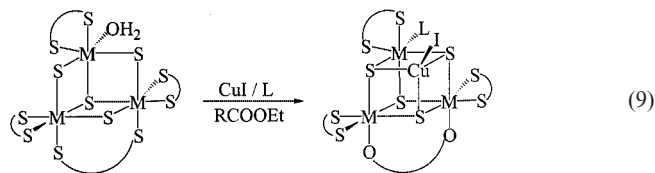
The trimolybdenum cluster  $[\text{Mo}_3\text{CoS}_4\text{Cp}'_3(\text{CO})]$  is formed in ca. 15% yield by heating  $[\text{Mo}_2\text{Co}_2(\mu_3\text{-S})_2(\mu_4\text{-S})\text{Cp}'_2(\text{CO})_4]$  in pyridine at 150 °C for 3 h, or by treatment of  $[\text{Mo}_2\text{Co}_2(\mu_3\text{-S})_4\text{Cp}'_2(\text{CO})_2]$  with a  $\text{CO}/\text{H}_2$  mixture in toluene at 250 °C (15–30% yield), as represented in Scheme 3.<sup>[24]</sup> The resulting  $\text{Mo}_3\text{Co}$  cluster appears to be a thermodynamic sink for the decomposition of the two  $\text{Mo}_2\text{Co}_2$  complexes. The intermetallic Mo–Mo and Mo–Co distances in this 16 electron  $\text{Mo}_3\text{Co}$  complex are ca. 0.09 and 0.027 Å longer than the corresponding distances in the 16 electron  $\text{Mo}_3\text{Ni}$  cluster. Finally, the cuboidal  $[\text{Mo}_3\text{FeS}_4\text{Cp}'_3(\text{SH})]$  compound is obtained in low yields from the reaction between the butterfly-type cluster  $[\text{Mo}_2\text{Fe}_2(\mu_3\text{-S})_2\text{Cp}'_2(\text{CO})_8]$  and thiophene at 150 °C in a pressure reactor.<sup>[24]</sup> The Mo–Mo and Mo–Fe distances in this cluster are 0.09 and 0.12 Å longer than the equivalent

distances in the  $[\text{Mo}_3\text{FeS}_4]^{4+}$  aquo cluster which also possesses 14 metal cluster electrons.

### $\text{M}_3\text{M}'\text{S}_4$ Clusters with Sulfur-Containing Ligands

In parallel to the development of the aqueous chemistry of the  $\text{M}_3\text{M}'\text{Q}_4$  complexes, a non-aqueous chemistry arises from inserting Cu into  $\text{M}_3\text{S}_4$  units derivatised with dithiophosphates  $[\text{dtp} = (\text{EtO})_2\text{PS}_2^-]$ . This was subsequently extended to other sulfur-containing ligands such as dithiocarbamates ( $\text{dtc} = \text{Et}_2\text{NCS}_2^-$ ) and dithiophosphinates ( $\text{R}_2\text{PS}_2^-$ ). These complexes are always prepared through  $[3 + 1]$  synthetic routes. The trimeric molybdenum and tungsten dithiophosphate precursors  $[\text{M}_3\text{S}_4\{(\text{EtO})_2\text{PS}_2\}_3(\mu_2\text{-(EtO)}_2\text{PS}_2)(\text{H}_2\text{O})]$  have been synthesised by reaction of  $\text{MoCl}_3 \cdot \text{H}_2\text{O}$  in ethanol or  $\text{EtOH}/\text{HCl}$  solutions.<sup>[88]</sup> The water molecule is easily replaced by other ligands such as dimethylformamide and pyridine. The dithiocarbamate and dithiophosphinate derivatives have been prepared by reduction of the disulfido  $\mu_2\text{-S}_2$  bridging ligand in  $[\text{Mo}_3(\mu_2\text{-S}_2)_3(\mu_3\text{-S})(\text{Et}_2\text{NCS}_2)_3]^+$  and  $[\text{Mo}_3(\mu_2\text{-S}_2)_3(\mu_3\text{-S})(\text{R}_2\text{PS}_2)_3]^-$  ( $\text{R} = \text{Et}, n\text{Pr}$ ) with triphenylphosphane to yield  $[\text{Mo}_3(\mu_2\text{-S})_3(\mu_3\text{-S})(\text{Et}_2\text{NCS}_2)_3(\mu_2\text{-Et}_2\text{NCS}_2)(\text{H}_2\text{O})]$  and  $[\text{Mo}_3(\mu_2\text{-S})_3(\mu_3\text{-S})(\text{R}_2\text{PS}_2)_3(\mu_2\text{-R}_2\text{PS}_2)(\text{py})]$ , respectively.<sup>[89–92]</sup> The structures of these trinuclear clusters are similar to other  $\text{M}_3\text{Q}_4$  trimers, with octahedral metal environments and with the bidentate chelating ligand occupying positions *trans* to the capping and one bridging sulfur atoms. The remaining coordination site is occupied by the sulfur atom of the bridging bidentate ligand for two of the metal atoms, and by a water or pyridine molecule for the remaining metal atom. This ligand arrangement gives rise to chirality.<sup>[93]</sup>

A series of heterodimetallic complexes with  $[\text{M}_3\text{CuS}_4]^{5+}$  cores and consequently 16 metal cluster electrons has been synthesised by treating  $[\text{M}_3\text{S}_4\{(\text{EtO})_2\text{PS}_2\}_3(\mu_2\text{-(EtO)}_2\text{PS}_2)(\text{L})]$  ( $\text{L} = \text{H}_2\text{O}, \text{CH}_3\text{CN}$ ) with CuI in organic solvents in the presence of various acetates, producing tetranuclear clusters of the general formula  $[\text{M}_3\text{CuS}_4\{(\text{EtO})_2\text{PS}_2\}_3(\mu_2\text{-O}_2\text{CR})\text{L}]$  ( $\text{R} = \text{CH}_3, \text{CF}_3, \text{CCl}_3$ ;  $\text{L} = \text{DMF}, \text{DMSO}, \text{py}, \text{CH}_3\text{CN}$ ), as shown in Equation (9).<sup>[70,94,95]</sup>



The  $\text{Mo}_3\text{CuS}_4$  dithiocarbamate and dithiophosphinate complexes  $[\text{Mo}_3\text{CuS}_4(\text{Et}_2\text{NCS}_2)_3(\mu_2\text{-Et}_2\text{NCS}_2)(\text{py})\text{I}]$  and  $[\text{Mo}_3\text{CuS}_4(\text{R}_2\text{PS}_2)_3(\mu_2\text{-R}_2\text{PS}_2)(\text{py})\text{I}]$  ( $\text{R} = \text{Et}, n\text{Pr}$ ) have also been prepared by reaction of the corresponding trimeric precursors with CuI in pyridine.<sup>[71,96,97]</sup> The presence of acetate ligands in the reaction media does not cause substitution of the bridging dithiocarbamate or dithiophosphinate, as is observed for the analogous dithiophosphate compound. This ligand environment provides these  $\text{M}_3\text{CuS}_4$

complexes with great stability towards air oxidation, in contrast to the equivalent aquo complexes.

The structures of several of these derivatives have been determined by single-crystal X-ray diffraction experiments. Intermetallic distances for some representative complexes are listed in Table 2. The coordination environment around the M atoms is pseudooctahedral, as observed for the trinuclear starting materials, although in the case of the dithiophosphate derivatives the bridging  $\mu_2\text{-(EtO)}_2\text{PS}_2^-$  ligand has been substituted for a bridging acetate ligand. The pseudotetrahedral Cu atom is coordinated to the iodine atom. The average M–M and M–Cu bond lengths are similar to those reported for the 16 metal electron aquo derivative  $[\text{Mo}_3\text{CuS}_4\text{Cl}(\text{Hnta})_3]^{2+}$ . However, the presence of a ligand bridging two molybdenum or tungsten atoms causes a shortening of this M–M bond length by ca. 0.08 Å, with concomitant lengthening of the M–Cu bonds by ca. 0.05–0.08 Å. The M–Cu distances are between 0.1 and 0.2 Å longer than the M–M' ( $\text{M}' = \text{Co}$  or  $\text{Ni}$ ) bond lengths observed for other 16 metal electron clusters.

### $\text{M}_3\text{M}'\text{S}_4$ Clusters with Phosphanes

A series of heterodimetallic clusters of molybdenum and tungsten with  $\text{M}_3\text{M}'\text{Q}_4$  ( $\text{Q} = \text{S}, \text{Se}$ ) units have been reported for  $\text{M}' = \text{Cu}$ , where the group-6 metal atom is coordinated to different bidentate phosphanes such as dmpe or dppe. Recent work in our group has shown that the procedures employed can also be extended to Co and Ni.<sup>[98]</sup> The preparation of these tetrametallic species has also been achieved through a  $[3 + 1]$  synthetic strategy, using the molecular clusters  $[\text{M}_3\text{Q}_4(\text{diphosphane})_3\text{X}_3]^+$  [ $\text{M} = \text{Mo}, \text{W}$ ;  $\text{Q} = \text{S}, \text{Se}$ ;  $\text{X} = \text{Cl}, \text{Br}$ ; diphosphane = 1,2-bis(dimethylphosphanyl)ethane (dmpe), 1,2-bis(diphenylphosphanyl)ethane (dppe)] as starting materials. The excision of polymeric  $\{\text{M}_3\text{Q}_7\text{X}_4\}_x$  phases with chalcogen-abstracting ligands such as phosphanes has proved to be a general method for the preparation of  $\text{M}_3\text{Q}_4$  incomplete cuboidal clusters having phosphanes as ancillary ligands.<sup>[54,99–101]</sup> The cationic  $[\text{M}_3\text{S}_4(\text{dmpe})_3\text{X}_3]^+$  trimers are obtained in high yields ( $> 90\%$ ) by excision of the corresponding  $\{\text{M}_3\text{S}_7\text{X}_4\}_x$  polymers with dmpe in refluxing acetonitrile.<sup>[102]</sup> The analogous dppe derivatives  $[\text{M}_3\text{S}_4(\text{dppe})_3\text{X}_3]^+$  are obtained in ca. 75% under similar reaction conditions. This synthetic method can also be extended to selenium, with typical yields of 50–65% for the  $[\text{M}_3\text{Se}_4(\text{dmpe})_3\text{X}_3]^+$  complexes and 67–85% for the  $[\text{M}_3\text{Se}_4(\text{dppe})_3\text{X}_3]^+$  compounds.<sup>[75,98,103,104]</sup> Alternatively, the  $[\text{M}_3\text{S}_4(\text{diphosphane})_3\text{X}_3]^+$  [diphosphane = dmpe, 1,2-bis(diethylphosphanyl)ethane (depe)] complexes can be obtained in 15–55% yields by treating the metal halides with NaHS in THF/methanol in the presence of an excess of dmpe or depe.<sup>[105–107]</sup> The synthesis of the (dppe)molybdenum derivatives in approximately 50% yield has been reported from the reaction of the molecular cluster  $[\text{Mo}_3\text{S}_7\text{X}_6]^{2-}$  ( $\text{X} = \text{Cl}, \text{Br}$ ) with dppe in methanol.<sup>[54]</sup> In addition, the  $[\text{M}_3\text{Se}_4(\text{dppe})_3\text{X}_3]^+$  cationic cluster can be obtained by excision of the polymeric precursor in molten



dppe, with an overall reaction yield of 40 and 62% for the Mo and W derivatives, respectively.<sup>[108]</sup> These  $[\text{M}_3\text{Q}_4(\text{diphosphane})_3\text{X}_3]^+$  complexes have one phosphorus atom *trans* to the capping sulfur atom and another *trans* to the bridging sulfur atom, as shown in Figure 4. This arrangement results in chiral complexes with an effective  $C_3$  symmetry. However, the nonstereospecificity of the reaction leads to racemic mixtures.

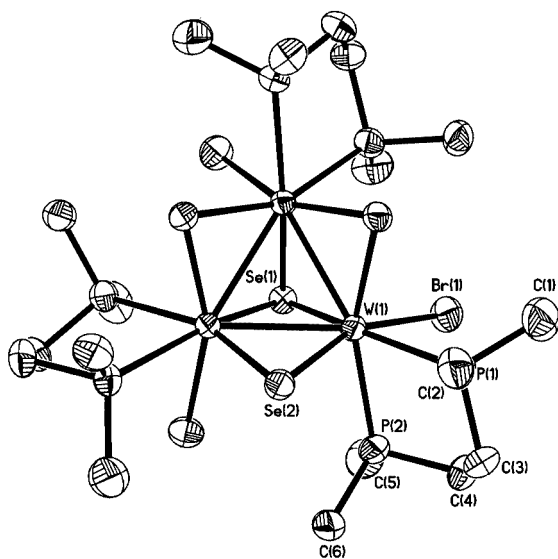
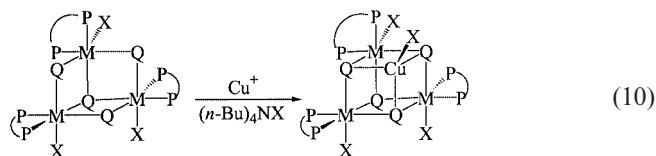


Figure 4. ORTEP representation of the  $[\text{W}_3\text{Se}_4(\text{dmpe})_3\text{Br}_3]^+$  cation; only the atoms in the asymmetric unit are labeled

The first attempt to introduce a first-row transition metal atom into an incomplete cuboidal  $\text{M}_3\text{S}_4$  unit was the reaction between the molybdenum(IV) trimer  $[\text{Mo}_3\text{S}_4\text{Cl}_4(\text{PEt}_3)_3 \cdot (\text{MeOH})_2]$  and  $[\text{Ni}(\text{cod})_2]$  in THF which afforded a pentanuclear  $\text{Mo}_3\text{Ni}_2\text{S}_4$  cluster instead of the expected  $\text{Mo}_3\text{Ni}$  cubane. X-ray structural analysis of this pentanuclear sulfido cluster revealed a square-pyramidal core with an  $\text{Mo}_2\text{Ni}_2$  base, an Mo atom at the vertex, and short intermetallic distances:  $d(\text{Mo}-\text{Mo}) = 2.65\text{--}2.67 \text{ \AA}$ ,  $d(\text{Mo}-\text{Ni}) = 2.50\text{--}2.67 \text{ \AA}$  and  $d(\text{Ni}-\text{Ni}) = 2.71 \text{ \AA}$ . An oxidation state assignment of  $\text{Mo}_3^{\text{IV}}\text{Ni}_2^0$  has been proposed based on the XPS spectra, suggesting that Ni incorporation into the Mo trimer occurs without changes in the metal oxidation states.<sup>[101]</sup>

Cubane-type  $\text{Mo}_3\text{CuQ}_4$  and  $\text{W}_3\text{CuS}_4$  clusters have been obtained by reaction of the trimers  $[\text{Mo}_3\text{Q}_4(\text{dmpe})_3\text{X}_3][\text{PF}_6]$  and  $[\text{W}_3\text{S}_4\text{X}_3(\text{dmpe})_3][\text{PF}_6]$  in THF with  $\text{CuX}$ , or with  $[\text{Cu}(\text{CH}_3\text{CN})_4][\text{PF}_6]$  in the presence of a tetrabutylammonium halide salt, to give the corresponding  $[\text{M}_3\text{CuQ}_4(\text{dmpe})_3\text{X}_4][\text{PF}_6]$  heterodimetallic tetramers, according to Equation (10).<sup>[5,75]</sup>



The products are air-stable and soluble in common organic solvents such as  $\text{CH}_2\text{Cl}_2$  and  $\text{CH}_3\text{CN}$ . Typical yields for the reaction range from 40 to 73%. The reaction takes place without overall changes in the oxidation states of the metal atoms, and these  $\text{M}_3\text{CuQ}_4$  clusters possess 16 electrons for metal-metal bonding. X-ray structural analysis reveals that there is no significant structural rearrangement on going from  $\text{M}_3\text{Q}_4$  to  $\text{M}_3\text{CuQ}_4$ , and in consequence the resulting heterodimetallic clusters are also chiral, although the product is again obtained as a racemic mixture. Metal-metal distances for some representative complexes are listed in Table 2. The M-M distances do not change significantly between molybdenum and tungsten, while the M-M bonds in the selenido derivatives are ca.  $0.06 \text{ \AA}$  longer than the corresponding distances in the sulfido complexes. The Mo-Cu bonds in the sulfido clusters are  $0.04 \text{ \AA}$  longer than the Mo-Mo distance, while the W-Cu bond is  $0.1 \text{ \AA}$  longer than the W-W distance. This distortion of the tetrametallic unit can be regarded as an elongation along the  $C_3$  axis through Cu, and is less pronounced for the selenido clusters in comparison to the analogous sulfido complexes. The average M-M and M-Cu bond lengths are similar to those reported for other  $\text{M}_3\text{CuQ}_4$  clusters having an identical metal electron population of  $16 e^-$ .

As previously mentioned, trinuclear  $[\text{M}_3\text{Q}_4(\text{diphosphane})_3\text{X}_3]^+$  (diphosphane = dmpe, dppe; X = Cl, Br) complexes can also incorporate atoms of other metals such as nickel or cobalt through reaction of the trimeric cations with  $[\text{Ni}(\text{cod})_2]$  or  $[\text{Co}_2(\text{CO})_8]$ .<sup>[98]</sup> Alternatively, an entry to these complexes through the  $[\text{Mo}_3\text{NiS}_4(\text{H}_2\text{O})_9\text{Cl}]\text{Cl}_3$  aquo ion has been proposed. Water substitution takes place by treating the solid aquo ion with dppe in methanol to afford  $[\text{Mo}_3\text{NiS}_4(\text{dppe})_3\text{Cl}_4]$  in 43% yield.<sup>[80]</sup> In contrast to the reactivity observed at the Ni site in the analogous cyclopentadienyl complexes, the Cl ligand attached to the Ni atom cannot be replaced by CO,  $\text{PMe}_3$  or  $\text{PMe}_2\text{Ph}$ . On the other hand, electrospray mass spectrometry of the Ni derivatives prepared by direct Ni insertion into the trimer  $[\text{M}_3\text{S}_4(\text{diphosphane})_3\text{X}_3]^+$  shows coordination of a solvent molecule to the heteroatom. This solvent molecule can then be substituted for a various N- and S-donor ligands.

### $\text{M}_3\text{M}'\text{S}_4$ Clusters with N-O Donor Tripodal Ligands

There is only one example of this type of clusters but it deserves special mention because it is the only case of an  $\text{Mo}_3\text{CuS}_4$  complex with a simple cubane structure and an odd number of metal cluster electrons ( $17 e^-$ ). The compound  $[\text{Mo}_3\text{CuS}_4(\text{tdci})_3\text{Br}]^{3+}$  [tdci = 1,3,5-trideoxy-1,3,5-tris(dimethylamino)-*cis*-inositol] was prepared in 55% yield by treating the trinuclear precursor  $[\text{Mo}_3\text{S}_4(\text{tdci})_3]^{4+}$  with copper metal in ethanol.<sup>[74]</sup> This synthetic route contrasts with the other procedure reported in non-aqueous solvents, in that Cu metal is used as starting material instead of a  $\text{Cu}^{\text{I}}$  halide, and this difference results in a change in the number of cluster metal electrons from 16 to 17. This complex has been structurally characterised and the intermetallic distances are listed in Table 2. The observed Mo-Mo and Mo-Cu distances in  $[\text{Mo}_3\text{CuS}_4(\text{tdci})_3\text{Br}]^{3+}$  are longer



than those found in all reported  $\text{Mo}_3\text{CuS}_4$  complexes having single cube structures and 16 metal electrons.

## Electronic Structure, Electrochemistry and Magnetism

### $\text{M}_2\text{M}'_2\text{S}_4$ Clusters

The most common ligand arrangement for the  $\text{M}_2\text{M}'_2$  cubane-type clusters results in a pseudooctahedral geometry around the 4d or 5d metal, M, and a pseudotetrahedral coordination environment for the first-row transition metal, M'. Harris et al. have developed a qualitative molecular orbital (MO) scheme for this system.<sup>[109]</sup> In this model, the metal M " $t_g$ " and the M' " $t_2$ " orbitals combine to form a set of six bonding and six antibonding orbitals, while the M " $e_g$ " and the M' " $e$ " orbitals remain nonbonding. This results in a total of ten metal-based MOs; four nonbonding low-lying MOs which are predominately M' in character and six bonding " $t$ " symmetry MOs of higher energy. Based on this model, a cluster metal electron count of 20 is expected to be necessary for a completely bonding metal  $\text{M}_2\text{M}'_2$  tetrahedron and any metal electrons in excess of this number are expected to occupy antibonding orbitals.

Table 1 lists intermetallic distances together with carbonyl and nitrosyl frequencies for some representative complexes with  $\text{Mo}_2\text{M}'_2\text{S}_4$  and  $\text{W}_2\text{M}'_2\text{S}_4$  central units. The strongest metal–metal interactions occur between the 4d or 5d metals in these complexes, and the weakest interactions are between the two 3d metals. These clusters can exist with metal electron counts between 16 and 22, although in the case of Cu and Ni only 22 electron systems have been reported to date. In the 20 electron clusters there are nominally six metal–metal bonds, and a bond order of one is assigned to the M'–M' bond. Differences in bond lengths between the Fe and Co complexes can be ascribed to the slightly larger covalent radius of Fe as compared to Co. All 20 electron clusters are diamagnetic.

The clusters with 16 or 18 metal electrons show a marked increase in the M'–M' distance. In the 18  $e^-$  systems, eight electrons will occupy the low-lying nonbonding orbitals leaving ten electrons to fill five metal–metal bonding orbitals. Different situations arise depending on the nature of these MOs, which may be highly delocalised over the tetrametallic core or localised between metal pairs. In the  $[\text{Mo}_2\text{Co}_2\text{S}_4\text{Cp}_2^{\text{Et}}\text{X}_2]$  (X = halogen) clusters, it appears that the electron density has been removed from the Co–Co bond, resulting in a long nonbonding  $\text{Co}\cdots\text{Co}$  distance. In the thiolato cluster  $[\text{Mo}_2\text{Co}_2\text{S}_4\text{Cp}_2^{\text{Et}}(\text{SPh})_2]$ , much less electron density appears to be removed from the Co–Co bond and an apparent bond order near 0.5 results.<sup>[21]</sup> These differences can be attributed to the differences in electronegativities and  $\pi$ -donor characteristics of the ligands on the Co atoms. These differences evidently affect the degree of localisation/delocalisation of the metal-based MOs involved in Co–Co bonding. In the 16 electron  $[\text{Mo}_2\text{Fe}_2\text{S}_4\text{Cp}^*_2\text{X}_2]$  cluster, the electron density is also preferentially removed

from the Fe–Fe bond.<sup>[20]</sup> The  $^1\text{H}$  NMR spectrum of this complex in  $\text{CDCl}_3$  showed a broad singlet at  $\delta = 1.81$  ppm, indicating the weak paramagnetic nature of this compound. On the other hand, the  $^1\text{H}$  NMR spectrum of the 18  $e^-$   $[\text{Mo}_2\text{Co}_2\text{S}_4\text{Cp}_2^{\text{Et}}\text{X}_2]$  (X = I, Br, Cl) complexes showed clear NMR peaks corresponding to those expected for  $\text{Cp}^{\text{Et}}$  ligands on diamagnetic clusters even though these complexes are paramagnetic both in solution and in the solid state. These  $[\text{Mo}_2\text{Co}_2]^{12+}$  halo compounds exhibit complex spin equilibria with thermally accessible  $S = 1, 2$  and 3 spin states and consequently there is no simple explanation for their apparently diamagnetic  $^1\text{H}$  NMR spectra. In contrast, the analogous thiolate cluster shows simple paramagnetism consistent with an  $S = 1$  spin state, which may simply mean that the  $S = 2$  state is not thermally accessible at the temperature studied since the thiolate ligands are better  $\pi$ -donors than halide ligands. No  $^1\text{H}$  NMR signal is observed for the  $[\text{Mo}_2\text{Co}_2\text{S}_4\text{Cp}_2^{\text{Et}}(\text{SPh})_2]$  thiolate cluster, as expected for a paramagnetic system. The differences in magnetic behaviour between the halide and thiolate  $[\text{Mo}_2\text{Co}_2]^{12+}$  complexes are not well understood and require further investigation.

The butterfly arrangement observed in the 16 and 18 metal electron clusters is also seen in the 21 and 22  $e^-$  complexes, and the M–M and M–M' distances correspond to single bonds (see Table 1). The M'–M' distance in the 22 metal electron complex is nonbonding, suggesting that the HOMO is an M'–M'  $\sigma^*$  antibonding orbital. The Co–Co bond lengths of 2.75 Å found in the 21  $e^-$  clusters are half-way between the fully bonded distance of 2.57 Å found in the 20 electron clusters and the nonbonding distance observed for the 22 electron systems, supporting the M'–M' antibonding character of the HOMO. This interpretation is also supported by the ESR spectrum of the  $[\text{Mo}_2\text{Co}_2\text{S}_4\text{Cp}_2^{\text{Et}}(\text{CO})_2]^-$  complex which is consistent with the odd electron being delocalised over two Co atoms, each with spin  $I = 7/2$ ; 13 of the expected 15 lines were observed, with the outer two being too weak.<sup>[26]</sup> Addition of another electron reduces the M'–M' bond order to zero, producing diamagnetic complexes.

Qualitative bonding schemes have also been developed for other  $\text{M}_2\text{M}'_2$  cubane sulfido clusters with different metal coordination environments to the ones previously discussed. Changes in the symmetry of the system result in different electron counts for the formation of intermetallic cluster bonds. For example, the Dahl group has developed an MO energy diagram for homometallic  $[\text{M}_4\text{S}_4\text{Cp}_4]$  clusters based on the cubic  $T_d$  symmetry of the metallic tetrahedron that makes it possible to predict and understand the changes in metal–metal bonding which accompany changes in the number of electrons.<sup>[110]</sup> The number of metal electrons required for a completely filled set of six M–M bonding orbitals ( $a_1 + e + t_2$ ) is 12. This bonding scheme is also assumed to be applicable to the relatively rare heterometallic  $[\text{M}_2\text{M}'_2\text{S}_4\text{Cp}_4]$  clusters. Although there are no structural data on these clusters, spectroscopic evidence suggests that the  $[\text{Mo}_2\text{Cr}_2\text{S}_4\text{Cp}^*_2\text{Cp}_2]$  complex with 12

cluster electrons has a cubane-type structure with presumably a fully bonded metal tetrahedron.<sup>[38]</sup>

Another combination of metal coordination geometries is found in the  $[\text{Mo}_2\text{Fe}_2\text{Cp}_2(\text{CO})_4]$  cluster with a square-pyramidal “ $\text{FeS}_3(\text{CO})_3$ ” fragment. Fenske–Hall calculations on this complex predict that a cluster electron count anywhere between 12 and  $16\text{ e}^-$  should lead to a completely bonding metal tetrahedron.<sup>[111]</sup> In the 18 electron  $[\text{Mo}_2\text{Fe}_2\text{Cp}_2(\text{CO})_4]$  compound, two electrons will occupy an Fe–Fe antibonding orbital and the long Fe–Fe distances observed in this complex agree with this prediction. On the other hand, the  $[\text{Mo}_2\text{Fe}_2\text{S}_4(\mu_2\text{-S}_2\text{CNEt}_2)(\text{S}_2\text{CNEt}_2)_4]$  complex, also with a pentacoordinate iron fragment (albeit trigonal-bipyramidal instead of square-pyramidal) and 15 metal cluster electrons, has a full set of six metal–metal bonds.

Finally, the  $[\text{M}_2\text{Cu}_2\text{S}_4(\text{S}_2\text{C}_2\text{H}_4)_2(\text{PPh}_3)_2]$  complexes with a pentacoordinate environment for the molybdenum and tungsten atoms that differs from the octahedral coordination found in the remaining  $\text{M}_2\text{M}'_2\text{S}_4$  clusters have the same butterfly-cubane geometry found in the octahedrally coordinated Mo and W complexes. Although no qualitative MO energy diagram of this system has been developed, the structural findings also agree with the existence of an antibonding HOMO localised between the two copper atoms, as theoretically predicted for the  $\text{M}_2\text{M}'_2\text{S}_4$  cyclopentadienyl derivatives.

A comparison of the IR spectra of the Mo clusters and their W analogues shows that the  $\nu_{\text{CO}}$  or  $\nu_{\text{NO}}$  values are lower for the tungsten clusters in all cases, indicating a higher back-donation for the heavier metal which is effectively more electron-rich. This is consistent with the electrochemical results. Cyclic voltammetry studies show that these systems undergo reversible or quasireversible conver-

sions between the 20, 21 and 22 metal electron species. The reported redox potentials for representative  $\text{M}_2\text{M}'_2$  compounds are listed in Table 3. The tungsten clusters are more difficult to reduce and easier to oxidise than their molybdenum analogues, which is also consistent with the tungsten complexes being more electron-rich.

### $\text{M}_3\text{M}'\text{Q}_4$ Clusters

Fenske–Hall MO calculations on  $\text{M}_3\text{M}'\text{S}_4$  complexes show the presence of a group of three strongly bonding cluster MOs ( $1\text{e}$  and  $1\text{a}_1$ ), a doubly degenerate  $\text{M}'$ -based bonding orbital ( $2\text{e}$ ), a group of three weakly antibonding cluster MOs ( $2\text{a}_1$  and  $3\text{e}$ ) and three strongly antibonding cluster MOs ( $4\text{e}$  and  $3\text{a}_1$ ).<sup>[112]</sup> In the clusters having electron counts of 14 and  $16\text{ e}^-$ , 12 metal electrons will occupy the cluster bonding orbitals and the weakly antibonding  $2\text{a}_1$  orbital, and two or four electrons will partially or fully occupy the  $3\text{e}$  HOMO. Metal electrons in excess of 16 will occupy strongly antibonding  $4\text{e}$  and  $3\text{a}_1$  cluster MOs.

This MO scheme is supported by magnetic susceptibility measurements on powdered samples of single crystals of  $[\text{Mo}_3\text{M}'\text{S}_4(\text{H}_2\text{O})_{10}][\text{pts}]_4 \cdot 7\text{H}_2\text{O}$  ( $\text{M}' = \text{Fe}, \text{Ni}$ ) which give effective moments of 2.78 B.M. at 2.16 K and 3.26 B.M. at 269.95 K for  $\text{M}' = \text{Fe}$  and 0.11 B.M. at 2.00 K and 1.26 B.M. at 260.7 K for  $\text{M}' = \text{Ni}$ .<sup>[65,113,114]</sup> These results are consistent with the presence of two unpaired electrons in the  $\text{Mo}_3\text{Fe}$  14 metal electron cluster and no unpaired electrons in the  $\text{Mo}_3\text{Ni}$  16 metal electron cluster. No ESR spectra could be observed for frozen solutions of  $[\text{Mo}_3\text{FeS}_4(\text{H}_2\text{O})_{10}]^{4+}$  in 2 M HCl or  $\text{HClO}_4$  at temperatures down to 4.2 K, in agreement with an  $S = 1$  ground state for this system. The magnetic susceptibility data for  $[\text{Mo}_3\text{M}'\text{S}_4(\text{H}_2\text{O})_{10}][\text{pts}]_4 \cdot 7\text{H}_2\text{O}$  ( $\text{M}' = \text{Fe}, \text{Ni}$ ) were analysed using the vector model formalism of Kambe and the

Table 3. Redox potentials [V vs. Fc] of some representative  $\text{Mo}_2\text{M}'_2\text{S}_4$  cubane-type clusters

Cluster <sup>[a]</sup>	No. of metal electrons	$E_{\text{red}}$	$E_{\text{ox}}$	Conditions	Correction	Ref.
$[\text{Mo}_2\text{Fe}_2\text{S}_4\text{Cp}^*_2\text{Cl}_2]$	16	−1.44 (rev.)		glassy carbon electrode THF/ $[\text{Bu}_4\text{N}][\text{ClO}_4]$	[b]	[20]
$[\text{Mo}_2\text{Fe}_2\text{S}_4\text{Cp}^{\text{Et}}_2(\text{NO})_2]$	20	−1.12 (rev.) −1.52 (rev.) −1.86 (rev.)	0.22 (irr.) 0.60 (irr.) 0.90 (irr.)	platinum electrode $\text{CH}_3\text{CN}/[\text{Bu}_4\text{N}][\text{PF}_6]$	[c]	[22]
$[\text{W}_2\text{Fe}_2\text{S}_4\text{Cp}^*_2(\text{NO})_2]$	20	−1.72 (rev.) −1.90 (rev.) −2.33 (qrev.)	0.08 (irr.) 0.40 (irr.) 1.14 (qrev.)	platinum electrode $\text{CH}_3\text{CN}/[\text{Bu}_4\text{N}][\text{PF}_6]$	[c]	[22]
$[\text{Mo}_2\text{Co}_2\text{S}_4\text{Cp}^{\text{Et}}_2(\text{CO})_2]$	20	−1.44 (rev.)	−0.20 (irr.) 0.22 (irr.)	platinum electrode $\text{CH}_3\text{CN}/[\text{Bu}_4\text{N}][\text{PF}_6]$	[c]	[22]
$[\text{Mo}_2\text{Ni}_2\text{S}_4\text{Cp}^*_2\text{Cp}_2]$	20	−1.47 (rev.) −2.30 (irr.)	−0.22 (rev.) 0.24 (rev.)	platinum electrode $\text{CH}_3\text{CN}/[\text{Bu}_4\text{N}][\text{BF}_4]$	[d]	[27]
$[\text{Mo}_2\text{Co}_2\text{S}_4\text{Cp}^{\text{Et}}_2(\text{NO})_2]$	22	−1.93 (rev.)	−0.60 (rev.)	platinum electrode $\text{CH}_3\text{CN}/[\text{Bu}_4\text{N}][\text{PF}_6]$	[c]	[22]
$[\text{W}_2\text{Co}_2\text{S}_4\text{Cp}^*_2(\text{NO})_2]$	22	−2.15 (rev.)	−0.47 (rev.)	platinum electrode $\text{CH}_3\text{CN}/[\text{Bu}_4\text{N}][\text{PF}_6]$	[c]	[22]
$[\text{Mo}_2\text{Ni}_2\text{S}_4\text{Cp}^*_2(\text{CO})_2]$	22	−1.65 (rev.) −2.18 (rev.)	0.15 (irr.) 0.35 (irr.)	platinum electrode $\text{CH}_3\text{CN}/[\text{Bu}_4\text{N}][\text{BF}_4]$	[d]	[27]
$[\text{Mo}_2\text{Cu}_2\text{S}_4(\text{C}_2\text{H}_4\text{S}_2)_2(\text{PPh}_3)_2]$	22	−1.22 (irr.)	—	platinum electrode $\text{CH}_2\text{Cl}_2/[\text{Bu}_4\text{N}][\text{ClO}_4]$	[e]	[31]
$[\text{W}_2\text{Cu}_2\text{S}_4(\text{C}_2\text{H}_4\text{S}_2)_2(\text{PPh}_3)_2]$	22	−1.66 (irr.)	—	platinum electrode $\text{CH}_2\text{Cl}_2/[\text{Bu}_4\text{N}][\text{ClO}_4]$	[e]	[31]

<sup>[a]</sup> Half-wave potential ( $E_{1/2}$ ) is given unless the wave is irreversible (irr.), in which case the peak potential ( $E_p$ ) is given. <sup>[b]</sup> Fc 0.56 V vs. SCE (THF/ $[\text{NBu}_4][\text{PF}_6]$ ); conversion into Fc approximate. <sup>[c]</sup> Fc 0.40 V vs. NHE.<sup>[22]</sup> <sup>[d]</sup> Fc 0.07 V vs.  $\text{Ag}[\text{NO}_3]/\text{Ag}$ .<sup>[27]</sup> <sup>[e]</sup> Fc 0.46 V vs. SCE ( $\text{CH}_2\text{Cl}_2/[\text{NBu}_4][\text{PF}_6]$ ); conversion into Fc approximate.

experimental data were fitted to a model with an  $\text{Mo}^{\text{IV}}\text{Mo}_2^{\text{III}}\text{M}'^{\text{II}}$  core. The ground state assignment agrees with the experimental results of  $^{57}\text{Fe}$ -Mössbauer spectroscopy, where the oxidation state of the iron atom in the  $\text{Mo}_3\text{Fe}$  cluster has been determined to be +2.39. The order of the binding energies of  $\text{Mo } 3d_{3/2}$  and  $\text{Mo } 3d_{5/2}$  for these tetranuclear clusters and their trinuclear  $\text{Mo}_3$  precursor have been obtained from X-ray photoelectronic spectra to give the following values:  $E(\text{Mo}_3) = 233.7, 230.7 \text{ eV}$ ;  $E(\text{Mo}_3\text{Fe}) = 233.1, 230.0 \text{ eV}$  and  $E(\text{Mo}_3\text{Ni}) = 233.3, 230.3 \text{ eV}$ . The fact that  $E(\text{Mo}_3) > E(\text{Mo}_3\text{M}')$  indicates a real charge transfer from the incorporated metal atom to the  $\text{Mo}_3$  trimer, in good agreement with the previous  $\text{Mo}^{\text{IV}}\text{Mo}_2^{\text{III}}\text{M}'^{\text{II}}$  metal oxidation state assignment.

A comparison of the bond lengths between the 14 and 16 metal electron  $\text{M}_3\text{M}'$  clusters with single-cube structures (see Table 2) does not show any clear relationship between the intermetallic distances and the number of metal electrons, in contrast to the general findings for  $\text{M}_2\text{M}'_2$  complexes. This fact can be attributed to the highly delocalised nature of the bond in the  $\text{M}_3\text{M}'$  system. On the other hand, significant differences are observed in the metal–metal bond lengths between clusters with identical  $\text{Mo}_3\text{M}'\text{S}_4$  cores and the same number of metal electrons, indicating that changes in the donor ability of the outer ligands have important effects on the electronic structure of the cluster.

Fenske–Hall calculations also show that the bonding/antibonding character of the middle group of cluster orbitals ( $2a_1$  and  $3e$ ) is affected by the relative energies of the  $\text{M}'$  and  $\text{M}_3$  fragment orbitals.<sup>[112]</sup> As the  $\text{M}'$  fragment orbitals increase in energy relative to the  $\text{Mo}_3$  fragment orbitals, they mix more strongly with the unoccupied  $\text{Mo}_3\text{S}_4$  fragment orbitals and as a result, the middle group of cluster orbitals becomes more bonding (or in this case, less antibonding). The energies of the  $\text{M}'$  fragment increase in the order  $\text{Cu} < \text{Ni} < \text{Co} < \text{Fe}$  and thus the antibonding character of the ( $2a_1$  and  $3e$ ) orbitals decrease according to the sequence  $\text{Cu} > \text{Ni} > \text{Co} > \text{Fe}$ . Consequently, the strength of the  $\text{M}-\text{M}'$  interaction increases in the order  $\text{Cu} < \text{Ni} < \text{Co} < \text{Fe}$ . This effect is seen in the calculated  $\text{M}-\text{M}'$  bond orders of 0.561 and 0.432 for  $[\text{Mo}_3\text{CoS}_4\text{Cp}'_3(\text{CO})]$  and  $[\text{Mo}_3\text{NiS}_4(\text{H}_2\text{O})_9(\text{CO})]^{4+}$ , respectively.

Discrete variational (DV)  $X\alpha$  calculations carried out on  $[\text{Mo}_3\text{M}'\text{S}_4(\text{H}_2\text{O})_{10}]^{4+}$  ( $\text{M}' = \text{Fe}, \text{Ni}$ ) complexes agree with the general picture of the bond provided by the Fenske–Hall scheme, except that the  $X\alpha$  method gives a HOMO with “a” symmetry for both the  $\text{Mo}_3\text{Fe}$  and the  $\text{Mo}_3\text{Ni}$  complexes.<sup>[65]</sup> In the case of nickel the HOMO symmetry matches the LUMO of small molecules such as carbon monoxide or ethylene, thus explaining the reactivity of the  $\text{Mo}_3\text{Ni}$  cluster towards these molecules. The absence of reactivity found for the iron complex has been attributed to the lack of symmetry matching between the  $\text{Mo}_3\text{Fe}$  cluster HOMO and the LUMO of these small molecules.

The only compounds with  $[\text{M}_3\text{M}'\text{Q}_4]$  cores and 17 metal cluster electrons to have been structurally characterised are those with  $\text{M} = \text{Mo}$ ,  $\text{M}' = \text{Cu}$  and  $\text{Q} = \text{S}$ , and two different structural types, isolated cube and double cubane, have

been identified. In all cases, the  $\text{Mo}-\text{Cu}$  distances are longer than those observed for the analogous 16 electron clusters. Extended Hückel MO calculations on isolated  $\text{Mo}_3\text{CuS}_4$  complexes suggest that the extra electron in the 17  $e^-$  cluster occupies a strongly antibonding  $\text{Mo}-\text{Mo}$  and  $\text{Mo}-\text{Cu}$  orbital, thus explaining the longer  $\text{Mo}-\text{Mo}$  and  $\text{Mo}-\text{Cu}$  distances observed for  $[\text{Mo}_3\text{CuS}_4(\text{tdci})_3\text{Br}]^{3+}$  [ $\text{tdci} = \text{cis-1,3,5-tris(dimethylamino)inositol}$ ].<sup>[74,77]</sup>

EPR studies on the 17 electron mixed-metal single-cubane cluster  $[\text{Mo}_3\text{CuS}_4(\text{H}_2\text{O})_{10}]^{4+}$ , generated by decomposition of the double cubane cluster complex  $\{[\text{Mo}_3\text{CuS}_4(\text{H}_2\text{O})_9]_2\}^{8+}$ , indicate that the complex is paramagnetic with  $S = 1/2$  and the hyperfine splitting is consistent with a metal oxidation state formulation of  $\text{Mo}_2^{\text{IV}}\text{Mo}^{\text{III}}\text{Cu}^{\text{I}}$  in which the paramagnetic centre is mainly located on one of the molybdenum atoms. The  $\text{Mo}^{\text{III}}$  site is not fixed at a specific position but moves over the three molybdenum sites at a rate of the order of  $10^7 \text{ s}^{-1}$ .<sup>[77]</sup> Extended Hückel MO calculations on the  $[\text{Mo}_3\text{CuS}_4(\text{H}_2\text{O})_{10}]^{4+}$  aquo ion agree with a large spin distribution on Mo, as observed experimentally.

The redox properties of these  $\text{M}_3\text{M}'\text{Q}_4$  complexes have been investigated by cyclic voltammetry and a list of selected potentials is presented in Table 4.

In general, the  $\text{M}_3\text{M}'$  clusters are easier to reduce than their  $\text{M}_2\text{M}'_2$  counterparts and, with the exception of the  $[\text{Mo}_3\text{NiS}_4(\text{dppe})_3\text{Cl}_4]$  complex which has a reversible oxidation wave at 0.2 V (vs. Fc), no oxidation processes have been reported for the  $\text{M}_3\text{M}'$  compounds, in contrast to the rich electrochemical activity found for the  $\text{M}_2\text{M}'_2$  clusters upon oxidation.<sup>[80]</sup> As found for the  $\text{M}_2\text{M}'_2$  system, the tungsten derivatives are more difficult to reduce than those of molybdenum. An interesting point arises when comparing the electrochemical behaviours of the tetrametallic  $\text{M}_3\text{M}'\text{Q}_4$  clusters with those of their trimeric  $\text{M}_3\text{Q}_4$  precursors. In the case of the Fe or Ni incorporation into the  $[\text{Mo}_3\text{S}_4]^{4+}$  aquo ion, the resulting  $[\text{Mo}_3\text{M}'\text{S}_4(\text{H}_2\text{O})_{10}]^{4+}$  ( $\text{M}' = \text{Fe}, \text{Ni}$ ) complexes are ca. 0.45 V more difficult to reduce than their precursor aquo trimers.<sup>[65]</sup> These observations suggest a formal oxidation state for the metals of  $\text{Mo}^{\text{IV}}\text{Mo}_2^{\text{III}}\text{M}'^{\text{II}}$ , in agreement with the Mössbauer and XPS experimental results. The three reduction waves can then be attributed to three monoelectronic processes, namely  $\text{Mo}^{\text{IV}}\text{Mo}_2^{\text{III}}\text{M}'^{\text{II}} \rightleftharpoons \text{Mo}^{\text{IV}}\text{Mo}_2^{\text{III}}\text{M}'^{\text{I}} \rightleftharpoons \text{Mo}^{\text{IV}}\text{Mo}_2^{\text{III}}\text{M}'^0 \rightleftharpoons \text{Mo}_3^{\text{III}}\text{M}'^0$ , taking into account that the peak potential for the third reduction of these  $\text{Mo}_3\text{Fe}$  and  $\text{Mo}_3\text{Ni}$  complexes is very close to that for the third reduction of the  $[\text{Mo}_3\text{S}_4]^{4+}$  aquo precursor in which  $\text{Mo}^{\text{IV}}\text{Mo}_2^{\text{III}}$  is reduced to  $\text{Mo}_3^{\text{III}}$ .

In contrast to the Fe and Ni findings, Cu insertion into the  $[\text{M}_3\text{Q}_4(\text{dmpe})_3\text{X}_3]^+$  trimers results in an anodic shift of the redox potential in the sulfides and selenides of both molybdenum and tungsten.<sup>[5,75]</sup> This fact, together with the  $\text{Mo}_2^{\text{IV}}\text{Mo}^{\text{III}}\text{Cu}^{\text{I}}$  oxidation state assignment of the 17 electron  $[\text{Mo}_3\text{CuS}_4]^{4+}$  aquo ion (based on EPR results) and close inspection of the redox potential values for the  $\text{Mo}_3\text{Cu}$  complexes and their  $\text{Mo}_3$  precursors (see Table 4), has led us to propose the following reduction mechanism:  $\text{Mo}_3^{\text{IV}}\text{Cu}^{\text{I}} \rightleftharpoons \text{Mo}_2^{\text{IV}}\text{Mo}^{\text{III}}\text{Cu}^{\text{I}} \rightleftharpoons \text{Mo}^{\text{IV}}\text{Mo}_2^{\text{III}}\text{Cu}^{\text{I}}$ . Note that the potential

Table 4. Redox potentials [V vs. Fc] of some representative  $M_3M'Q_4$  cubane-type clusters and their trinuclear  $M_3S_4$  precursors

Cluster <sup>[a]</sup>	No. of metal electrons	$E_{red}$	Conditions	Correction	Ref.
$[Mo_3S_4(H_2O)_9]^{4+}$	6	−0.54 (qrev.) −1.10 (qrev.) −1.83 (irr.)	glassy carbon electrode $CH_3CN/[Bu_4N][PF_6]$	[b]	[65]
$[Mo_3FeS_4(H_2O)_{10}]^{4+}$	14	−1.00 (irr.) −1.56 (irr.) −1.90 (irr.)	glassy carbon electrode $CH_3CN/[Bu_4N][PF_6]$	[b]	[65]
$[Mo_3NiS_4(H_2O)_{10}]^{4+}$	16	−1.00 (irr.) −1.57 (irr.) −1.81 (irr.)	glassy carbon electrode $CH_3CN/[Bu_4N][PF_6]$	[b]	[65]
$[Mo_3S_4(dmpe)_3Cl_3]^+$	6	−1.13 (qrev.) −1.82 (irr.)	platinum electrode $CH_3CN/[Bu_4N][PF_6]$	[c]	[102]
$[Mo_3CuS_4(dmpe)_3Cl_4]^+$	16	−0.81 (qrev.) −1.19 (irr.)	platinum electrode $CH_3CN/[NBu_4][PF_6]$	[d]	[5]
$[Mo_3S_4(dmpe)_3Br_3]^+$	6	−1.00 (qrev.) −1.64 (irr.)	platinum electrode $CH_3CN/[Bu_4N][PF_6]$	[c]	[102]
$[Mo_3CuS_4(dmpe)_3Br_4]^+$	16	−0.73 (qrev.) −1.08 (irr.)	platinum electrode $CH_3CN/[Bu_4N][PF_6]$	[d]	[5]
$[Mo_3Se_4(dmpe)_3Br_3]^+$	6	−0.98 (irr.) −1.31 (irr.) −1.64 (irr.)	platinum electrode $CH_3CN/[Bu_4N][PF_6]$	[c]	[75]
$[Mo_3CuSe_4(dmpe)_3Br_4]^+$	16	−0.73 (qrev.) −1.31 (irr.) −1.56 (irr.)	platinum electrode $CH_3CN/[Bu_4N][PF_6]$	[c]	[75]

<sup>[a]</sup> Half-wave potential ( $E_{1/2}$ ) is given unless the wave is irreversible (irr.), in which case the peak potential ( $E_p$ ) is given. <sup>[b]</sup> Fc 0.094 V vs.  $Ag^+/Ag$ .<sup>[65]</sup> <sup>[c]</sup> Fc 0.44 V vs.  $Ag^+/Ag$ .<sup>[102]</sup> <sup>[d]</sup> Fc 0.5 V vs.  $Ag^+/Ag$ .<sup>[5]</sup>

values for the second reduction process of the  $Mo_3Cu$  complexes are similar to the peak potential of the first bielectronic wave found for the sulfide trimers, where  $Mo_3^{IV}$  is reduced to  $Mo_2^{IV}Mo^{III}$ . They are also similar to the peak potential of the second monoelectronic wave observed in the trinuclear selenides, where  $Mo_2^{IV}Mo^{III}$  is reduced to  $Mo^{IV}Mo_2^{III}$ . A similar mechanism could be tentatively extended to the  $W_3CuS_4$  complexes. In general the selenido clusters are more easily reduced than the analogous sulfides.

## Properties and Applications

In this last section we highlight some properties of these  $M_2M'_2S_4$  and  $M_3M'Q_4$  transition metal chalcogenido clusters that make these complexes useful as materials with potential technological applications. We have chosen these properties based on our own interests in catalysis, nonlinear optics and the capability of these complexes to form supramolecular adducts.

### Catalysis

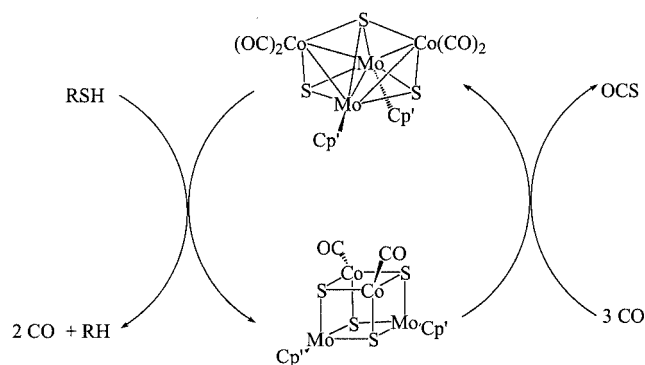
The only molecular clusters of the type discussed in this microreview that have proved to resemble the industrial HDS heterogeneous catalyst are the  $Mo_2Co_2S_x$  ( $x = 3, 4$ ) complexes. As described in a previous section,  $[Mo_2Co_2(\mu_3-S)_2(\mu_4-S)Cp'_2(CO)_4]$  reacts with thiols at temperatures of several hundred degrees below that used in the HDS of petroleum feed stocks to give the cubane cluster  $[Mo_2Co_2S_4Cp'_2(CO)_2]$  in almost quantitative yields together with the corresponding hydrocarbon. No molecular re-

arrangement or alkene formation is observed in the course of the reaction. This fact, together with the stereospecificity of the reaction, indicates homolytic cleavage of the C–S bond.<sup>[25,115]</sup> The reaction of  $[Mo_2Co_2S_3Cp'_2(CO)_4]$  with the thiolate  $MeC_6H_4S^-$  was studied at  $-60^\circ C$  by NMR spectroscopy and it provides the first insight into the mechanism of desulfurisation. Initially, the thiolate ion binds a cobalt atom to form a red adduct. An increase of the temperature to  $-24^\circ C$  causes a transformation of this red adduct to a green compound in which the thiolate bridges the Co–Mo bond. Desulfurisation occurs upon heating this bridged adduct under reflux conditions in deuterated MeCN to produce  $[D_1]toluene$  ( $MeC_6H_4D$ ) plus the radical anion  $[Mo_2Co_2(\mu_3-S)_4Cp'_2(CO)_2]^-$ , again supporting the idea of homolytic cleavage of the C–S bond.<sup>[25]</sup>

This  $Mo_2Co_2S_3$  cluster also cleaves the C–S bond in thiols by an apparent free radical mechanism. The kinetics of thiol desulfurisation are first-order in both cluster and thiol concentration. When the reaction product  $[Mo_2Co_2(\mu_3-S)_4Cp'_2(CO)_2]$  is heated at  $150^\circ C$  with CO at 69 atm, a 20% conversion into  $[Mo_2Co_2(\mu_3-S)_2(\mu_4-S)Cp'_2(CO)_4]$  and OCS is obtained. The combination of the sulfur abstraction reaction and the regeneration of  $[Mo_2Co_2S_3Cp'_2(CO)_4]$  constitutes a cycle for catalytic carbonyl desulfurisation of organic sulfides, as represented in Scheme 7.<sup>[21,25,41,115]</sup>

The cluster  $[Mo_2Co_2(\mu_3-S)_4Cp_2^{Et}(CO)_2]$  reacts with good sulfur donors such as thiiranes and thietanes to give the organic hydrocarbons that result from their hydrodesulfurisation, together with an insoluble black solid for which a polymeric structure of  $[Mo_2Co_2(\mu_3-S)_4Cp_2^{Et}]$  cubes linked together by sulfur bridges has been proposed.<sup>[116]</sup>





Scheme 7. Catalytic desulfurisation cycle of organic sulfides

$[\text{Mo}_2\text{Co}_2(\mu_3\text{-S})_4\text{Cp}_2^{\text{Et}}(\text{SPh})_2]$ , obtained by oxidation of the carbonyl starting material cluster, was used to model the sulfur-bridged polymer. When  $[\text{Mo}_2\text{Co}_2(\mu_3\text{-S})_4\text{Cp}_2^{\text{Et}}(\text{SPh})_2]$  is treated with  $\text{H}_2$  ( $13.4 \times 10^5$  Pa)/CO ( $13.4 \times 10^5$  Pa) at  $130^\circ\text{C}$ , the carbonyl cluster  $[\text{Mo}_2\text{Co}_2(\mu_3\text{-S})_4\text{Cp}_2^{\text{Et}}(\text{CO})_2]$  is regenerated and gives PhSSPh as the sole organic product. Furthermore, a catalytic cycle for the conversion of PhSH to PhSSPh with the  $\text{Mo}_2\text{Co}_2\text{S}_4$  cluster as catalyst is feasible.<sup>[21]</sup> It is interesting to point out that these  $\text{Mo}_2\text{Co}_2\text{S}_x$  ( $x = 3, 4$ ) clusters are capable of cleaving C–S bonds at temperatures several hundred degrees below that used in the industrial heterogeneous hydrodesulfurisation process, suggesting that C–S bond activation is not the rate-determining step in the industrial process, but rather the removal of sulfur from the surface of the catalyst.

The cluster  $[\text{Mo}_2\text{Co}_2(\mu_3\text{-S})_2(\mu_4\text{-S})\text{Cp}'_2(\text{CO})_4]$  has been supported on alumina and subjected to temperature-programmed decomposition under hydrogen. The activity and selectivity of this  $\text{MoCoS}/\text{Al}_2\text{O}_3$  system for thiophene hydrodesulfurisation are similar to those of conventionally prepared catalysts under similar reaction conditions. Spectroscopic characterisation of the cluster-derived catalyst suggests that the clusters undergo oxidation by the surface upon loss of the organic ligands.<sup>[117]</sup>

The uptake of CO is often used as a measure of the HDS activity of a heterogeneous catalyst. The fact that several  $\text{M}_3\text{M}'\text{Q}_4$  complexes react with CO supports the idea that these clusters may be functional models in homogeneous HDS catalysis.<sup>[63]</sup> The ability of the heterometal atoms in the  $[\text{M}_3\text{M}'\text{Q}_4]^{n+}$  ( $\text{M}' = \text{Fe}, \text{Co}, \text{Ni}, \text{Cu}$ ) aquo ions to bind CO has been correlated with the number of metal cluster electrons. The  $\text{Mo}_3\text{CoS}_4$  and  $\text{M}_3\text{NiQ}_4$  cubes with 15 and 16 metal electrons react with CO to afford the  $[\text{Mo}_3\text{CoS}_4(\text{H}_2\text{O})_9(\text{CO})]^{4+}$ ,  $[\text{Mo}_3\text{NiQ}_4(\text{H}_2\text{O})_9(\text{CO})]^{4+}$  and  $[\text{W}_3\text{NiS}_4(\text{H}_2\text{O})_9(\text{CO})]^{4+}$  cationic clusters, which are more stable than their starting aquo ions. In the case of nickel, the presence of chloride ions in the reaction media precludes formation of the carbonyl adduct, and CO is replaced by  $\text{Cl}^-$  on addition of concentrated HCl to  $[\text{M}_3\text{NiQ}_4(\text{H}_2\text{O})_9(\text{CO})]^{4+}$ . Coordination of CO to  $[\text{Mo}_3\text{CoS}_4(\text{H}_2\text{O})_{10}]^{4+}$  is reversible, and bubbling nitrogen through  $[\text{Mo}_3\text{CoS}_4(\text{H}_2\text{O})_9(\text{CO})]^{4+}$  regenerates the starting aquo ion. The  $[\text{Mo}_3\text{CuS}_4(\text{H}_2\text{O})_{10}]^{5+}$  cluster, which has the

same 16 metal electron count as the Ni complexes, reacts with CO in a different manner to produce the trinuclear  $[\text{Mo}_3\text{S}_4]^{4+}$  aquo ion plus  $[\text{Cu}(\text{CO})]^+$ . As observed for the cobalt system, bubbling of nitrogen regenerates the starting aquo cluster. On the other hand, the  $[\text{Mo}_3\text{FeS}_4(\text{H}_2\text{O})_{10}]^{4+}$  and  $[\text{Mo}_3\text{CuS}_4(\text{H}_2\text{O})_{10}]^{4+}$  clusters, with 14 and 17 metal cluster electrons, respectively, do not react with CO.<sup>[48]</sup>

The IR spectra of  $[\text{M}_3\text{NiS}_4(\text{H}_2\text{O})_9(\text{CO})]^{4+}$  show CO stretching bands at  $2077\text{ cm}^{-1}$  for  $\text{M} = \text{Mo}$  and  $2045\text{ cm}^{-1}$  for  $\text{M} = \text{W}$ . IR spectra of heterogeneous NiWS catalysts after CO uptake display a CO band at  $2090\text{ cm}^{-1}$ , suggesting that there are differences in the chemical environment between the nickel atoms in the NiMS heterogeneous catalyst and in the  $[\text{M}_3\text{NiS}_4(\text{H}_2\text{O})_9(\text{CO})]^{4+}$  aquo ions. The structural characterisation of  $[\text{Mo}_3\text{NiS}_4\text{Cp}'_3\text{L}]^+$  compounds in which the nickel atom is coordinated to organic sulfur- or nitrogen-containing ligands (L), do not indicate any activation of the C–S or C–N bonds, as reported in a previous section. In addition, the reaction between  $[\text{Mo}_3\text{NiS}_4\text{Cp}'_3\text{L}]^+$  and benzothiophene/quinoline at 30 bar of  $\text{H}_2$  and  $130^\circ\text{C}$  does not reveal the formation of any of the expected hydrodesulfurisation or hydrodenitrogenation products.<sup>[67]</sup> This lack of HDS activity has been attributed to the low electron density on Ni, based on quantum mechanical calculations.<sup>[112]</sup> However, the limited backbonding to CO, a consequence of the low electron density on the heterometal, is also observed in the industrial MNiS catalysts. Further investigations are needed to understand these observations.

One of the key problems in the hydrodesulfurisation of light oil is the low reactivity of 4-methyldibenzothiophene and 4,6-dimethyldibenzothiophene, since the methyl groups hinder the approach of sulfur to the active sites of the catalyst. In order to overcome this limitation,  $[\text{Mo}_3\text{S}_4(\text{H}_2\text{O})_9]^{4+}$  and  $[\text{Mo}_3\text{NiS}_4(\text{H}_2\text{O})_9\text{Cl}]^{3+}$  have been loaded into zeolites in the hope that the acidic properties of zeolites might be capable of activating the alkyl group(s) in the thiophenic derivatives as the cluster core promotes the desulfurisation reaction. The  $\text{Mo}_3\text{S}_4$  and  $\text{Mo}_3\text{NiS}_4$  complexes have been incorporated into zeolites (NaY, HUSY, NaH $\beta$ , Na mordenite and KL) by aqueous ion-exchange without destruction of the zeolite structure.<sup>[118–120]</sup> The trinuclear cluster remains virtually intact after ion exchange. On the other hand, partial decomposition of the NiMo cluster to  $\text{Ni}^{2+}$  and the  $\text{Mo}_3\text{S}_4$  trimer has been observed after ion exchange. The HDS activity of benzothiophene is significantly affected by the zeolite structure and the best results are found for NaY or KL. The catalysts prepared by incorporation of the nickel heterodimetallic cluster were more active in the HDS reaction than those prepared by ion exchange of the  $\text{Mo}_3\text{S}_4$  cluster with nickel nitrate solutions in the zeolites. The effectiveness of employing the MoNi mixed cluster suggests some similarities between the structure of the active sites and that of the  $\text{Mo}_3\text{Ni}$  heterodimetallic cluster.

Recent work in our group shows that the  $[\text{Mo}_3\text{CuS}_4(\text{dmpe})_3\text{Cl}_4]^+$  cationic cluster is a useful catalyst for the cyclopropanation of diazo compounds. The reaction of 1-diazo-5-penten-2-one in dichloromethane solutions un-

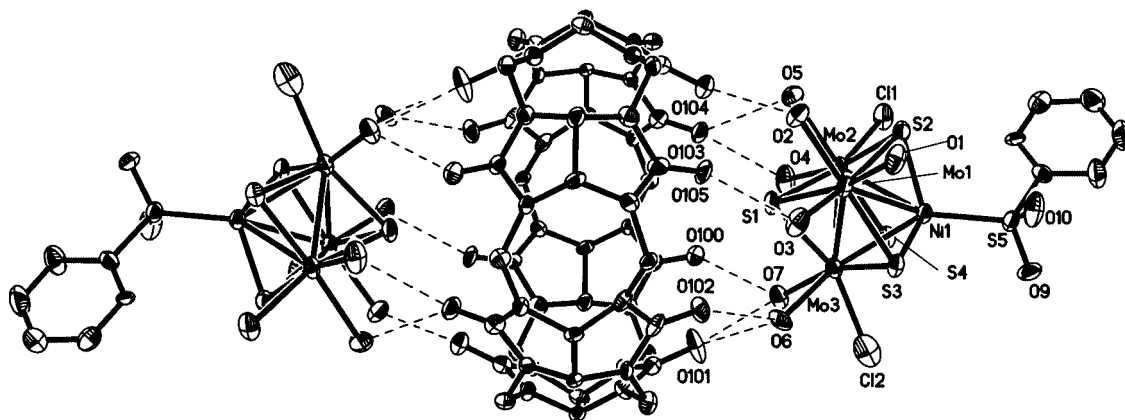


Figure 5. Drawing of the  $[\{\text{Mo}_3[\text{Ni}(\text{PhSO}_2)]\text{S}_4(\text{H}_2\text{O})_{7.83}\text{Cl}_{1.17}\}_2(\text{C}_{36}\text{H}_{36}\text{N}_{24}\text{O}_{12})]^{3.66+}$  supramolecular adduct with partial atom-numbering scheme

der reflux conditions for 3 d affords the cyclopropanation product bicyclo[3.1.0]pentan-2-one in yields greater than 95%.<sup>[121]</sup>

### Nonlinear Optics

The optical-limiting merit of transition metal clusters has attracted much interest recently because these compounds combine the advantages of the presence of heavy atoms with structural versatility of the coordination environment. The clusters  $[\text{M}_3\text{CuS}_4(\text{dmpe})_3\text{X}_4]^+$  ( $\text{X} = \text{Cl}, \text{Br}$ ) as well as their trinuclear precursors  $[\text{M}_3\text{Q}_4(\text{diphosphane})_3\text{X}_3]^+$  (diphosphane = dmpe, dppe) are all efficient optical limiters.<sup>[5,108]</sup> A large ratio of the effective excited-state cross section ( $\sigma_{\text{eff}}$ ) to ground-state absorption cross section ( $\sigma_0$ ) is one criterion for assessing potential as optical limiters. Values of  $\sigma_{\text{eff}}/\sigma_0$  for these trinuclear and tetranuclear clusters lie within an order of magnitude (from 1.1 to 12), suggesting a common power-limiting mechanism, possibly purely thermal in origin. The threshold-limiting fluence in these optical limiters decreases on proceeding from the tetranuclear cluster to its trinuclear precursor and from the tungsten-containing to its molybdenum-containing analogue.

### Formation of Supramolecular Adducts

The  $\text{M}_3\text{M}'\text{S}_4$  aquo ions yield supramolecular compounds on reaction with macrocyclic ligands such as cucurbituril (cuc).<sup>[122,123]</sup> In cases where  $\text{M}'$  is a first-row transition metal, this ligand forms stable compounds with cations such as  $[\text{Mo}_3\text{NiS}_4(\text{H}_2\text{O})_7\text{Cl}_3]^+$ ,  $[\text{Mo}_3\text{NiS}_4(\text{H}_2\text{O})_8\text{Cl}_2]^{2+}$  and  $[\text{Mo}_3\text{NiS}_4(\text{H}_2\text{O})_9(\text{PhSO}_2)]^{3+}$ .<sup>[124,125]</sup> The typical arrangement (cluster)(cucurbituril)(cluster) is shown in Figure 5 for the latter derivative. The driving force for the crystallisation process is the formation of several complementary hydrogen bonds between the C=O groups and the water molecules coordinated to the cluster, and as a result, addition of cucurbituril is often used as a method to facilitate crystallisation of cuboidal aquo ions.

This entry to supramolecular chemistry also allows the development of host–guest chemistry. This is illustrated by

the crystallisation of the supramolecular adduct  $\{[\text{Mo}_3\text{NiS}_4(\text{H}_2\text{O})_8\text{Cl}_2](\text{pyH}^+\text{Cuc})\}\text{Cl}_3 \cdot 14 \cdot 5\text{H}_2\text{O}$  with a pyridinium cation inside the cucurbituril cavity.

### Acknowledgments

This work was supported by the Spanish Dirección General de Enseñanza Superior e Investigación Científica (DGESIC, research project PB98-1044), Generalitat Valenciana (CTIDIB/2002/330) and Fundació Caixa Castelló-UJI (research project P1-1B2001-07).

- [1] E. I. Stiefel, K. Matsumoto, *Transition Metal Sulfur Chemistry*, ACS Symposium Series, Honolulu (Hawaii), **1995**.
- [2] V. P. Fedin, J. Czyżniewska, R. Prins, T. Weber, *Appl. Catal. A* **2001**, *213*, 123–132.
- [3] T. Weber, R. Prins, R. A. van Santen, *Transition Metal Sulfides – Chemistry and Catalysis*, Eds. Kluwer, Dordrecht, **1998**.
- [4] Q.-F. Zhang, Y.-N. Xiong, T.-S. Lai, W. Ji, X.-Q. Xin, *J. Phys. Chem. B* **2000**, *104*, 3446–3449.
- [5] M. Feliz, J. M. Garriga, R. Llugar, S. Uriel, M. G. Humphrey, N. T. Lucas, M. Samoc, B. Luther-Davies, *Inorg. Chem.* **2001**, *40*, 6132–6138.
- [6] S.-B. Yu, A. B. Watson, *Chem. Rev.* **1999**, *99*, 2353–2377.
- [7] S. B. Yu, M. Droegge, B. Segal, S. H. Kim, T. Sanderson, A. D. Watson, *Inorg. Chem.* **2000**, *39*, 1325–1328.
- [8] R. H. Holm, P. Kennepohl, E. I. Solomon, *Chem. Rev.* **1996**, *96*, 2239–2314.
- [9] J. B. Howard, D. C. Rees, *Chem. Rev.* **1996**, *96*, 2965–2982.
- [10] S. M. Malinak, D. Coucouvanis, *Prog. Inorg. Chem.* **2001**, *49*, 599–662.
- [11] B. E. Schimth, *Adv. Inorg. Chem.* **1999**, *47*, 160–218.
- [12] P. Braunstein, R. Jacky, *Metal Clusters in Chemistry* (Eds.: P. Braunstein, L. A. Oro, P. R. Raithby), Wiley-VCH Verlag GmbH, Weinheim, Germany, **1999**, vol. 2, p. 616–677.
- [13] S. Shi, W. Ji, J. P. Lang, X. Q. Xin, *J. Phys. Chem.* **1994**, *98*, 3570–3572.
- [14] S. Shi, W. Ji, S. H. Tang, J. P. Lang, X. Q. Xin, *J. Am. Chem. Soc.* **1994**, *116*, 3615–3616.
- [15] T. Shibahara, *Coord. Chem. Rev.* **1992**, *123*, 73–147.
- [16] T. Saito, *Adv. Inorg. Chem.* **1996**, *44*, 45.
- [17] R. Hernandez-Molina, A. G. Sykes, *J. Chem. Soc., Dalton Trans.* **1999**, 3137–3148.
- [18] R. Hernandez-Molina, M. N. Sokolov, A. G. Sykes, *Acc. Chem. Res.* **2001**, *34*, 223–230.
- [19] M. Hidai, S. Kuwata, Y. Mizobe, *Acc. Chem. Res.* **2000**, *33*, 46–52.

- [20] H. Kawaguchi, K. Yamada, S. Ohnishi, K. Tatsumi, *J. Am. Chem. Soc.* **1997**, *119*, 10871–10872.
- [21] M. A. Mansour, M. D. Curtis, J. W. Kampf, *Organometallics* **1997**, *16*, 3363–3370.
- [22] M. A. Mansour, M. D. Curtis, J. W. Kampf, *Organometallics* **1997**, *16*, 275–284.
- [23] T. R. Halbert, S. A. Cohen, E. I. Stiefel, *Organometallics* **1985**, *4*, 1689–1690.
- [24] M. D. Curtis, U. Riaz, O. J. Curnow, J. W. Kampf, A. L. Rheingold, B. S. Haggerty, *Organometallics* **1995**, *14*, 5337–5343.
- [25] S. H. Druker, M. D. Curtis, *J. Am. Chem. Soc.* **1995**, *117*, 6366–6367.
- [26] M. D. Curtis, S. H. Druker, L. Goossen, J. W. Kampf, *Organometallics* **1997**, *16*, 231–235.
- [27] M. D. Curtis, P. D. Williams, W. M. Butler, *Inorg. Chem.* **1988**, *27*, 2853–2862.
- [28] H. Brunner, R. Grabl, J. Wachter, B. Nuber, M. L. Ziegler, *J. Organomet. Chem.* **1990**, *393*, 119–129.
- [29] J. Xu, J. Qian, Q. Wei, *Inorg. Chim. Acta* **1989**, *164*, 55–58.
- [30] H. Brunner, N. Janietz, J. Wachter, T. Zahn, M. L. Ziegler, *Angew. Chem. Int. Ed. Engl.* **1985**, *24*, 133–135.
- [31] N. Y. Zhu, Y. Zheng, X. Wu, *J. Chem. Soc., Chem. Commun.* **1990**, 780–781.
- [32] J. Wu, N. Zhu, S. Du, X. Wu, J. Lu, *Inorg. Chim. Acta* **1991**, *185*, 181–185.
- [33] N. Zhu, R. Wu, X. Wu, *Acta Crystallogr., Sect. C* **1991**, *47*, 1537–1539.
- [34] H. Brunner, W. Meier, J. Wachter, E. Guggolz, T. Zahn, M. L. Ziegler, *Organometallics* **1982**, *1*, 1107–1113.
- [35] M. R. Dubois, D. L. Dubois, M. C. VanDerveer, R. C. Haltiwanger, *Inorg. Chem.* **1981**, *20*, 3064–3071.
- [36] M. D. Curtis, P. D. Williams, *Inorg. Chem.* **1983**, 2661–2662.
- [37] R. A. Schunn, C. J. Fritch, C. T. Prewitt, *Inorg. Chem.* **1966**, *5*, 892–899.
- [38] H. Brunner, H. Kauermann, J. Wachter, *J. Organomet. Chem.* **1984**, 265, 189–198.
- [39] U. Riaz, O. J. Curnow, M. D. Curtis, *J. Am. Chem. Soc.* **1994**, *116*, 4357–4363.
- [40] H. Brunner, J. Wachter, *J. Organomet. Chem.* **1982**, *240*, C41–C44.
- [41] M. A. Mansour, M. D. Curtis, J. W. Kampf, *Organometallics* **1995**, *14*, 5460–5462.
- [42] H. Brunner, H. Kauermann, J. Wachter, *Angew. Chem. Int. Ed. Engl.* **1983**, *22*, 549–550.
- [43] K. F. Miller, A. E. Bruce, J. L. Corbin, S. Wherland, E. I. Stiefel, *J. Am. Chem. Soc.* **1980**, *102*, 5102–5104.
- [44] W.-H. Pan, T. Chandler, J. H. Enemark, E. I. Stiefel, *Inorg. Chem.* **1984**, *23*, 4265–4269.
- [45] S. A. Cohen, E. I. Stiefel, *Inorg. Chem.* **1985**, *24*, 4657–4662.
- [46] N. Y. Zhu, Y. Zheng, X. Wu, *Inorg. Chem.* **1990**, *29*, 2705–2707.
- [47] T. Ikada, S. Kuwata, Y. Mizobe, M. Hidai, *Inorg. Chem.* **1998**, *37*, 5793–5797.
- [48] R. Hernandez-Molina, A. G. Sykes, *Coord. Chem. Rev.* **1999**, *187*, 291–302.
- [49] I. J. McLean, R. Hernandez-Molina, M. N. Sokolov, M. S. Seo, A. V. Virovets, M. R. J. Elsegood, W. Clegg, A. G. Sykes, *J. Chem. Soc., Dalton Trans.* **1998**, 2557–2562.
- [50] T. Shibahara, H. Akashi, H. Kuroya, *J. Am. Chem. Soc.* **1986**, *108*, 1342–1343.
- [51] F. A. Cotton, Z. Dori, R. Llusar, W. Schwotzer, *J. Am. Chem. Soc.* **1985**, *107*, 6734–6735.
- [52] T. Shibahara, H. Kuroya, *Polyhedron* **1986**, *5*, 357–361.
- [53] P. Kathirgamanathan, M. Martinez, A. G. Sykes, *J. Chem. Soc., Chem. Commun.* **1985**, 953–954.
- [54] V. P. Fedin, M. N. Sokolov, Y. V. Mironov, B. A. Kolesov, S. V. Tkachev, V. Y. Fedorov, *Inorg. Chim. Acta* **1990**, *167*, 39–45.
- [55] R. Hernandez-Molina, D. N. Dybtsev, V. P. Fedin, M. R. J. Elsegood, W. Clegg, A. G. Sykes, *Inorg. Chem.* **1998**, *37*, 2995–3001.
- [56] V. P. Fedin, M. N. Sokolov, A. G. Sykes, *J. Chem. Soc., Dalton Trans.* **1996**, 4089–4092.
- [57] V. P. Fedin, M. N. Sokolov, A. V. Virovets, N. V. Podberezskaya, V. Y. Fedorov, *Inorg. Chim. Acta* **1998**, *269*, 292–296.
- [58] R. Hernandez-Molina, M. R. J. Elsegood, W. Clegg, A. G. Sykes, *J. Chem. Soc., Dalton Trans.* **2001**, 2173–2178.
- [59] T. Shibahara, H. Akashi, M. Yamasaki, K. Hashimoto, *Chem. Lett.* **1991**, 689–692.
- [60] T. Shibahara, M. Yamasaki, H. Akashi, T. Katayama, *Inorg. Chem.* **1991**, *30*, 2693–2699.
- [61] T. Shibahara, H. Akashi, H. Kuroya, *J. Am. Chem. Soc.* **1988**, *110*, 3313–3314.
- [62] T. Shibahara, G. Sakane, M. Maeyama, H. Kobashi, T. Yamamoto, T. Watase, *Inorg. Chim. Acta* **1996**, *251*, 207–225.
- [63] I. Schmidt, J. Hyldoft, J. Hjortkjaer, C. J. Jacobsen, *Acta Chem. Scand.* **1996**, *50*, 871–874.
- [64] P. W. Dimmock, G. J. Lamprecht, A. G. Sykes, *J. Chem. Soc., Dalton Trans.* **1991**, 955–959.
- [65] T. Shibahara, G. Sakane, Y. Naruse, K. Taya, H. Akashi, A. Ichimura, H. Adachi, *Bull. Chem. Soc. Jpn.* **1995**, *68*, 2769–2782.
- [66] T. Shibahara, S. Mochida, G. Sakane, *Chem. Lett.* **1993**, 89–92.
- [67] K. Herbst, M. Monari, M. Brorson, *Inorg. Chem.* **2002**, *41*, 1336–1338.
- [68] K. Herbst, L. Dahlenburg, M. Brorson, *Inorg. Chem.* **2001**, *40*, 1989–1992.
- [69] H. Akashi, T. Shibahara, *Inorg. Chim. Acta* **2000**, *300*–302, 572–580.
- [70] X. Wu, S. Lu, L. Zu, Q. Wu, J. Lu, *Inorg. Chim. Acta* **1987**, *133*, 39–42.
- [71] H. Diller, H. Keck, W. Kuchen, D. Mootz, R. Wiskemann, *Z. Naturforsch., Teil B* **1993**, *48*, 291–296.
- [72] Y. Zheng, H. Zhan, X. Wu, *Acta Crystallogr., Sect. C* **1989**, *45*, 1990–1992.
- [73] S. Lu, H. Chen, J. Huang, Q. Wu, Q. Sun, J. Li, J. Lu, *Inorg. Chim. Acta* **1995**, *232*, 43–50.
- [74] K. Hegetschweiler, M. Wörh, M. D. Meienberger, R. Nesper, H. W. Schmalle, R. D. Hancock, *Inorg. Chim. Acta* **1996**, *250*, 35–47.
- [75] R. Llusar, S. Uriel, C. Vicent, *J. Chem. Soc., Dalton Trans.* **2001**, 2813–2818.
- [76] M. Nasreldin, Y.-J. Li, E. M. Frank, A. G. Sykes, *Inorg. Chem.* **1994**, *33*, 4283–4289.
- [77] R. Miyamoto, S. Kawata, M. Iwaizumi, H. Akashi, T. Shibahara, *Inorg. Chem.* **1997**, *36*, 542–546.
- [78] C. A. Routledge, M. Humanes, Y.-J. Li, G. Sykes, *J. Chem. Soc., Dalton Trans.* **1994**, 1275–1282.
- [79] T. Shibahara, T. Asano, G. Sakane, *Polyhedron* **1991**, *10*, 2351–2352.
- [80] D. Masui, Y. Ishii, M. Hidai, *Bull. Chem. Soc. Jpn.* **2000**, *73*, 931–938.
- [81] H. Akashi, T. Shibahara, *Inorg. Chim. Acta* **1998**, *282*, 50–54.
- [82] P. Vergamini, H. Vahrenkamp, L. Dahl, *J. Am. Chem. Soc.* **1971**, *93*, 6327–6329.
- [83] B. Rink, M. Brorson, *Organometallics* **1999**, *18*, 2309–2313.
- [84] K. Herbst, M. Monari, M. Brorson, *Inorg. Chem.* **2001**, *40*, 2979–2985.
- [85] W. Beck, W. Danzer, G. Thiel, *Angew. Chem. Int. Ed. Engl.* **1973**, *12*, 582–583.
- [86] R. E. Cramer, K. Yamada, H. Kawaguchi, K. Tatsumi, *Inorg. Chem.* **1996**, *35*, 1743–1746.
- [87] K. Herbst, B. Rink, L. Dahlenburg, M. Brorson, *Organometallics* **2001**, *20*, 3655–3660.
- [88] J. Q. Huang, J. L. Huang, M. Y. Shang, S. F. Lu, X. T. Lin, Y. H. Lin, M. D. Huang, H. H. Zhuang, J. X. Lu, *Pure Appl. Chem.* **1988**, *60*, 1185–1192.
- [89] H. Zimmermann, K. Hegetschweiler, T. Keller, V. Gramlich, H. Schmalle, W. Petter, W. Schneider, *Inorg. Chem.* **1991**, *30*, 4336–4341.

- [90] M. J. Mayor-López, J. Weber, K. Hegetschweiler, M. D. Meienberger, F. Joho, S. Leoni, R. Nesper, G. J. Reiss, W. Frank, B. A. Kolesov, V. P. Fedin, V. E. Fedorov, *Inorg. Chem.* **1998**, *37*, 2633–2644.
- [91] H. Keck, W. Kuchen, J. Mathow, B. Meyer, D. Mootz, H. Wunderlich, *Angew. Chem. Int. Ed. Engl.* **1981**, *20*, 975–976.
- [92] H. Keck, W. Kuchen, J. Mathow, B. Meyer, D. Mootz, H. Wunderlich, *Angew. Chem. Int. Ed. Engl.* **1982**, *21*, 929–930.
- [93] R. Hernandez-Molina, M. Sokolov, W. Clegg, P. Esparza, A. Mederos, *Inorg. Chim. Acta* **2002**, *331*, 52–58.
- [94] H. Zhan, Y. Zheng, X. Wu, J. Lu, *Inorg. Chim. Acta* **1989**, *156*, 277–280.
- [95] Y. Zheng, H. Zhan, X. Wu, J. Lu, *Transition Met. Chem.* **1989**, *14*, 161–164.
- [96] S. F. Lu, H. B. Chen, J. Q. Huang, Q. J. Wu, Q. L. Sun, J. Li, J. X. Lu, *Inorg. Chim. Acta* **1995**, *232*, 43–50.
- [97] [97a] H. Diller, H. Keck, H. Wunderlich, W. Kuchen, *J. Organomet. Chem.* **1995**, *489*, 123–127. [97b] H. Diller, H. Keck, A. Kruse, W. Kuchen, D. Mootz, R. Wiskemann, *Z. Naturforsch., Teil B* **1993**, *48*, 548–554.
- [98] M. Feliz, R. Llusar, S. Uriel, C. Vicent, unpublished results.
- [99] T. Saito, N. Yamamoto, T. Yamagata, H. Imoto, *Chem. Lett.* **1987**, 2025–2028.
- [100] F. A. Cotton, P. A. Kibala, M. Matusz, C. S. McCaleb, R. B. W. Sandor, *Inorg. Chem.* **1989**, *28*, 2623–2630.
- [101] T. Saito, Y. Kajitani, T. Yamagata, H. Imoto, *Inorg. Chem.* **1990**, *29*, 2951–2955.
- [102] F. Estevan, M. Feliz, R. Llusar, J. A. Mata, S. Uriel, *Polyhedron* **2001**, *20*, 527–535.
- [103] V. P. Fedin, M. N. Sokolov, A. O. Gerasko, A. V. Virovets, N. V. Podberezskaya, V. Y. Fedorov, *Inorg. Chim. Acta* **1991**, *187*, 81–90.
- [104] V. P. Fedin, M. N. Sokolov, K. G. Myakishev, O. A. Gerasko, V. Y. Fedorov, *Polyhedron* **1991**, *10*, 1311–1317.
- [105] F. A. Cotton, R. Llusar, *Polyhedron* **1987**, *6*, 1741–1745.
- [106] F. A. Cotton, R. Llusar, C. T. Eagle, *J. Am. Chem. Soc.* **1989**, *111*, 4332–4338.
- [107] F. A. Cotton, S. K. Mandal, *Inorg. Chim. Acta* **1992**, *192*, 71–79.
- [108] M. Feliz, R. Llusar, S. Uriel, C. Vicent, M. G. Humphrey, N. T. Lucas, M. Samoc, B. Luther-Davies, *Inorg. Chim. Acta*, accepted for publication.
- [109] S. Harris, *Polyhedron* **1989**, *8*, 2843–2882.
- [110] Trinh-Toan, B. K. Teo, J. A. Ferguson, T. J. Meyer, L. F. Dahl, *J. Am. Chem. Soc.* **1977**, *99*, 408–416.
- [111] S. Harris, *Inorg. Chem.* **1987**, *26*, 4278–4285.
- [112] C. S. Bahn, A. Tan, S. Harris, *Inorg. Chem.* **1998**, *37*, 2770–2778.
- [113] H. Akashi, T. Shibahara, N. Uryu, *Inorg. Chim. Acta* **1997**, *261*, 53–57.
- [114] P. W. Dimmock, P. E. Dickson, A. G. Sykes, *Inorg. Chem.* **1990**, *29*, 5120–5125.
- [115] U. Riaz, O. J. Curnow, M. D. Curtis, *J. Am. Chem. Soc.* **1994**, *116*, 4357–4363.
- [116] M. D. Curtis, S. H. Druker, *J. Am. Chem. Soc.* **1997**, *119*, 1027–1036.
- [117] M. D. Curtis, J. E. Penner-Hahn, J. Schwank, O. Barait, D. J. McCabe, L. Thompson, G. Waldo, *Polyhedron* **1988**, *7*, 2411–2420.
- [118] T. Tastumi, M. Tanaguchi, H. Ishige, Y. Ishii, T. Murata, M. Hidai, *Appl. Surf. Sci.* **1997**, *121/122*, 500–504.
- [119] M. Taniguchi, D. Imamura, H. Ishige, Y. Ishii, T. Murata, M. Hidai, T. Tatsumi, *J. Catal.* **1999**, *187*, 139–150.
- [120] M. Taniguchi, Y. Ishii, T. Murata, T. Tatsumi, M. Hidai, *J. Chem. Soc., Chem. Commun.* **1995**, 2533–2534.
- [121] R. Llusar, J. Pérez-Prieto, M. Barberis, M. Feliz, C. Vicent, S. Uriel, unpublished results.
- [122] M. N. Sokolov, A. V. Virovets, D. N. Dybtsev, A. Gerasko, V. P. Fedin, R. Hernandez-Molina, W. Clegg, A. G. Sykes, *Angew. Chem. Int. Ed.* **2000**, *39*, 1659–1661.
- [123] V. P. Fedin, A. V. Virovets, M. N. Sokolov, D. N. Dybtsev, O. A. Gerasko, W. Clegg, *Inorg. Chem.* **2000**, *39*, 2227–2230.
- [124] V. Fedin, V. Gramlich, M. Worle, T. Weber, *Inorg. Chem.* **2001**, *40*, 1074–1077.
- [125] M. N. Sokolov, R. Henández-Molina, D. N. Dybtsev, E. V. Chubarova, S. F. Solodovnikov, N. V. Pervukhina, C. Vicent, R. Llusar, V. Fedin, *Z. Anorg. Allg. Chem.* **2002**, *628*, 2335–2339.

Received October 15, 2002

[102569]